Linalool's Multifaceted Antimicrobial Potential: Unveiling its Antimicrobial Efficacy and Immunomodulatory Role Against *Saprolegnia parasitica*

Tao Tang[1], *Weiming Zhong*[1], *Puyu Tang*[3], *Rongsi Dai*[1], *Jiajing Guo*[2]* and *Zhipeng Gao*[1]**

[1] Hunan Engineering Technology Research Center of Featured Aquatic Resources Utilization, Fisheries College, Hunan Agricultural University
Changsha, Hunan, 410128, China
E-mail: gaozhipeng627@163.com

[2] Hunan Agriculture Product Processing Institute, Hunan Academy of Agricultural Sciences
Changsha, Hunan, 410125, China
E-mail: guojiajing1986@163.com

[3] State Key Laboratory of Freshwater Ecology and Biotechnology, Institute of Hydrobiology, Chinese Academy of Sciences
Wuhan, Hubei, 430072, China

Abstract

Saprolegnia parasitica (*S. parasitica*) is one of the most virulent oomycete species in freshwater aquatic environments, causing severe saprolegniasis and leading to significant economic losses in the aquaculture industry. Thus far, the prevention and control of saprolegniasis face a shortage of medications. Linalool, a natural antibiotic alternative found in various essential oils, exhibits promising antimicrobial activity against a wide range of pathogens. In this study, the specific role of linalool in protecting *S. parasitica* infection at both *in vitro* and *in vivo* levels was investigated. Linalool showed multifaceted anti-oomycetes potential by both of antimicrobial efficacy and immunomodulatory efficacy. For *in vitro* test, linalool exhibited strong anti-oomycetes activity and mode of action included: (1) Linalool disrupted the cell membrane of the mycelium, causing the intracellular components leak out; (2) Linalool prohibited ribosome function, thereby inhibiting protein synthesis and ultimately affecting mycelium growth. Surprisingly, meanwhile we found the potential immune protective mechanism of linalool in the *in vivo* test: (1) Linalool enhanced the complement and coagulation system which in turn activated host immune defense and lysate *S. parasitica* cells; (2) Linalool promoted wound healing, tissue repair, and phagocytosis to cope with *S. parasitica* infection; (3) Linalool positively modulated the immune response by increasing the abundance of beneficial Actinobacteriota; (4) Linalool stimulated the production of inflammatory cytokines and chemokines to lyse *S. parasitica* cells. In all, our findings showed that linalool possessed multifaceted anti-oomycetes potential which would be a promising natural antibiotic alternative to cope with *S. parasitica* infection in the aquaculture industry.

Keywords: *Saprolegnia parasitica*, linalool, anti-oomycetes mechanism, immune protective mechanism, antibiotic alternative

1. Introduction

Saprolegniasis is one of the most serious oomycete diseases in the aquaculture industry all over the world, infecting a wide host range (fish, crustaceans, amphibians, and their eggs.) with a conspicuous symptom (grayish-white cotton wool-like covering on the surface of host)[1, 2]. Oomycete infections lead to significant economic losses and serious damage to natural ecosystems[1]. As the infection intensifies, saprolegniasis can cause muscle ulceration, compromised immune system, respiratory problems, secondary infection, and finally result in host death[3]. *Saprolegnia*, *Achlya*, and *Leptolegnia* are key pathogens responsible for Saprolegniasis outbreaks[4], among them, *Saprolegnia* is proven to be the most virulent[5, 6]. *S. parasitica*, *S. ferax*, *S. delica*, and *S. diclina* are the main pathogens causing saprolegniasis[7], as a highly virulent group belonging to the phylum Oomycota, *S. parasitica* serves as the primary species in fish infections[8].

In the past, malachite green was highly effective in controlling *saprolegnia* infections, however, it has been banned worldwide for its carcinogenic and toxicological effects, which led to a sharp re-emergence of *Saprolegnia* infections in aquaculture industry[9]. Recently, various methods have been established to deal with *S. parasitica* infections, mainly including physical (water quality management, temperature control, and so on), chemical (hydrogen peroxide, natural antimicrobial compounds, and so on), and biological (probiotics, antagonistic microbe, and so on) methods[10]. Among these, antibiotics have served as the primary therapeutic and prophylactic tools for Saprolegniasis management in aquaculture. However, their overuse and abuse have resulted in antibiotic resistance among various aquatic pathogens[11]. Therefore, the increasing need for sustainable and eco-friendly strategies to combat *saprolegnia* infections has driven research into natural antimicrobial agents, due to their advantages in terms of avoiding antibiotic resistance issues, health safety, and ecological sustainability[12].

Plant extracts regulate specific and non-specific immunity, promoting immune responses and playing a crucial role in improving production performance, enhancing

antioxidant capacity, combating viruses, preventing diseases, and improving gut health[13]. This immunomodulatory function is mainly attributed to the secondary metabolites found in plants, such as flavonoids, polysaccharides, lactones, alkaloids, diterpenoids, and glycosides. These secondary metabolites can not only directly enhance immune capacity but also balance the gut microbiota and strengthen the intestinal mucosal barrier. After ingestion, plant extracts improve the immune defense mechanisms of intestinal epithelial cells, resist diseases caused by pathogenic microorganisms, and effectively enhance the body's resistance to pathogen infections[14]. In our earlier studies, the anti-oomycetes activities of 12 plant essential oils (EOs) and 5 of their major compounds (linalool, pinene, limonene, myrcene, and terpinene) were evaluated, and we found that linalool was one of the strongest anti-oomycetes compounds and selected for further study[15]. Linalool, a monoterpene alcohol found in various EOs, has shown promising antimicrobial activity against a wide range of pathogens[16]. Our groups and other research teams have reported that linalool exhibits antimicrobial activity against bacteria such as *Escherichia coli*[12], *Listeria monocytogenes*[17], *Elizabethkingia miricola*, *Streptococcus pyogenes*[18], *Pseudomonas fragi*[19], *staphylococcus aureus*[20], *Brochothrix thermosphacta*[21] and *Aeromonas hydrophila*[22], as well as against oomycetes like *Colletotrichum lagenarium*[23] and *Phytophthora capsici*[24], and fungi including *Aspergillus flavus*[25], *Penicillium citrinum*, *Chaetomium globosum*[26], *Colletotrichum gloesporioides*, *Fusarium oxysporum*[27], *Botrytis cinerea*[28] and *Candida albicans*[29].

In our previous study, we found that linalool exhibited strong antimicrobial activity against *S. ferax*[15], while whether it is also a promising agent against *S. parasitica*, another key virulent pathogen for *Saprolegniasis*is is still unknown, and the detailed mechanism, especially the *in vivo* immune mechanism induced by linalool remains poorly understood. Thus, in this study we focused on *S. parasitica* and aimed to investigate the specific role of linalool in protecting *S. parasitica* infection at both of *in vitro* and *in vivo* level by using different technologies, including *in situ* fluorescence observation, microstructure observation, Molecular Docking, AlphaFold2,

transcriptome profiling, histological examinations, gut microbiota analysis, and deep bioinformatics analysis. We believe this study will shed light on the antimicrobial activity and mode of action of linalool against *S. parasitica*, and contribute to the development of novel antibiotic alternative strategies to cope with *S. parasitica* infection in aquaculture industry.

2. Results

2.1 The *in vitro* anti-oomycete activity of linalool against *S. parasitica* CQT2

Figure 1A illustrated the anti-oomycetes activities of EOs and their major components against *S. parasitica* CQT2. Notably, linalool and the EO extracted from daidai flowers were particularly effective in restraining mycelium growth.

After adding 5 μL of resazurin dye, when the color of the wells turned to pink, the linalool concentration in the first non-pink well corresponded to the MIC. The culture liquid in the hole where no mycelium growth was seen was marked onto the plate and incubated at 25 °C for 7 days. The well with the lowest linalool concentration and no mycelium growth was identified as MFC. Linalool exhibited the MIC and MFC of 0.025% and 0.025% (v/v, 0.216 mg/mL) against spores, respectively (Figure 1B). Besides, both the MIC and MFC against mycelium growth were 0.05% (v/v, 0.432 mg/mL) and 0.1% (v/v, 0.864 mg/mL), respectively. Various linalool doses were examined against *S. parasitica* CQT2 on linalool-containing plates to evaluate their impact on inhibiting mycelium growth. As shown in Figure 1C-D, the findings indicated the anti-oomycetes activity of linalool against *S. parasitica* CQT2 was dose-dependent. Figure 1E displayed mycelium growth on PDA plates under varying linalool concentrations. The viability of mycelium following linalool treatment was assessed using a PI staining assay, where non-viable (dead) mycelium appeared red after PI uptake. Untreated mycelium showed no detectable red fluorescent, indicating 100% viability. In contrast, distinct red fluorescent mycelium was observed after linalool treatment at both MIC and 2×MIC levels (Figure 1F).

2.2 Effects of linalool on cell membrane damage of *S. parasitica* CQT2

Confocal microscopy using amphiphilic styryl dye FM4-64 has been employed to study endocytosis and vesicle trafficking in living fungal hyphae, while SYTO 9, a fluorescent nucleic acid stain, is widely used in microbiology, particularly in fluorescence microscopy, to evaluate bacterial viability[30]. The *in situ* fluorescence observations were displayed in Figure 2A, with linalool treatment for 0 minutes, the mycelium structure remained undamaged, and the red and green fluorescence showed an even distribution. After 2 min, red fluorescence started appearing within the mycelium, accompanied by the entry of the styryl dye FM4-64, indicating damage to the cell membrane. As the duration of linalool treatment increased, the intensity of red fluorescence within the mycelium also increased, indicating a rise in the number of mycelial cell deaths along with severe damage to the cell membrane. When examined by SEM, the mycelium exhibited a smooth and intact surface in the control group (Figure 2B), while in the treated groups (Figure 2C), it appeared wrinkled, deformed, and shrunken (Red dashed quadrilateral). When examined by TEM, the untreated mycelium cell exhibited clear and intact ultrastructure in the cell membrane, cell wall, mitochondria, and rough endoplasmic reticulum (Figure 2D). However, after treatment with linalool, the cell membrane was wrinkled and seriously damaged, and mitochondria began to dissolve (Figure 2E). As shown in Figure 2F-G, the cell membrane structure disappeared, the cell wall became thinner, and some exhibited severe deformation and bending. Vacuoles appeared in the cytoplasm, and mitochondria and rough endoplasmic reticulum ruptured and dissolved (red circles). No intact organelles were present within the cytoplasm.

As shown in the GO classification analysis (Figure 2H), the cellular components were distributed across 8 groups, with "cell part" and "membrane part" being the most prevalent. The differentially expressed genes (DEGs) associated with the intrinsic component of the membrane were identified and categorized into four classes: linked to ribosome function, involved in DNA/RNA function, connected to signal transduction and regulation, and pertaining to cell metabolism (Figure 2I). GO classification analysis revealed a significant number of differentially expressed genes (DEGs) associated with

the intrinsic components of the membrane. This finding is further supported by observations from scanning electron microscopy (SEM) and transmission electron microscopy (TEM), which provide consistent evidence aligning with the GO classification analysis results. Therefore, the cell membrane may be a potential target for linalool.

2.3 The *in vitro* anti-oomycete mechanisms revealed by transcriptome analysis

As shown in Figure S1A-B, a total of 4142 differentially expressed genes (DEGs) were discovered between the control and treatment groups, with 2016 showing upregulation and 2108 downregulation. Figure 2H presented the Gene Ontology (GO) analysis, providing a comprehensive evaluation of the functional aspects of genes and their products. These DEGs were categorized into 20 GO categories, with 6 associated with biological activities, where cellular and metabolic functions had the most DEGs. There were also 6 molecular function categories, with catalytic activity and binding containing the majority of DEGs. Additionally, Figure S1C demonstrated the results of Kyoto Encyclopedia of Genes and Genomes (KEGG) annotation, revealing 10 metabolic (M) pathways, 2 environmental information processing (EIP) pathways, 2 cellular processes (CP), and 5 genetic information processing (GIP).

2.3.1 The ribosome biogenesis and protein synthesis of *S. parasitica* were prohibited by linalool

Figure 3A-B displayed the results of GO enrichment analysis, revealing the top 20 biological processes that differed significantly between the control and treated groups. Notably, in Figure 3B, the downregulated biological processes are highlighted, and remarkably, 19 of them were associated with "ribosome", such as ribosome biogenesis, ribonucleoprotein complex biogenesis, pre ribosome, and small-subunit process some. In addition, KEGG enrichment analysis in Figure 3C revealed that "Ribosome biogenesis in eukaryotes" was the most enriched pathway, aligning with the GO enrichment analysis results mentioned earlier. The pathway of ribosome biogenesis in eukaryotes (Figure 3D) showed that linalool influenced DNA transcription, tRNA transport, rRNA processing and maturation (5.8S, 18S, and 25S), and the biogenesis

203 and assembly of ribosome subunits (40S and 60S) in the cell, which might lead to the
204 reduction of *S. parasitica* growth. We found that many DEGs related to ribosome
205 biogenesis (Figure 3D) and RNA polymerase (Figure 3E) are down expressed. Figure
206 3A highlighted the upregulated biological processes, and notably, 11 of them were
207 linked to "amino acids", such as the sulfur amino acid, L-phenylalanine, alpha-amino
208 acid, tyrosine, and homocysteine. Amino acids serve essential roles within the cell,
209 acting as both the foundational components for synthesizing new proteins and as
210 precursors for various metabolic processes[31].

211 The results of GO enrichment analysis and KEGG enrichment analysis suggested
212 that linalool might interact with specific domains of the ribosome, potentially affecting
213 its structure and function. To determine whether linalool could bind to ribosome-
214 associated upstream proteins in *S. parasitica*, molecular docking was conducted to
215 explore the specific binding proteins of linalool with the ribosome. The binding energy
216 of linalool was -6.2 kcal/mol with NOP, -4.8 kcal/mol with SNU13, and -5.0 kcal/mol
217 with DKC1 (Table S1). Consequently, NOP1 was selected as the receptor protein for
218 subsequent molecular docking. Figure 3F illustrated the tertiary structure of ribosomal
219 protein NOP1. Linalool formed hydrogen bonds with glutamic acid (Glu155) and
220 phenylalanine (Phe156) of NOP1 while exhibiting hydrophobic interactions with
221 alanine (Ala181), arginine (Arg182), valine (Val201), and isoleucine (Ile209) (Figure
222 3G). In summary, this interference may hinder the ribosome's ability to execute normal
223 biological processes, such as protein synthesis, thereby impacting the growth and
224 reproduction of oomycetes.

225 **2.3.2 The global metabolisms of *S. parasitica* were regulated by linalool**

226 In KEGG enrichment analysis, we found that 6 processes were associated with
227 metabolic pathways, such as cysteine and methionine metabolism, starch and sucrose
228 metabolism, and sulfur metabolism. Moreover, metabolic pathways were the most
229 annotated pathway which was in line with the results of KEGG annotation analysis. As
230 many changes were linked to metabolism, the Interactive Pathways Explorer (iPath)
231 was employed to comprehend the global differential metabolic response in *S. parasitica*

232 CQT2 (Figure 3I) which identified that linalool affects the global metabolic regulation
233 of *S. parasitica* CQT2.

234 **2.3.3 ABC transporters of *S. parasitica* were affected by linalool**

235 Some other important pathways were significantly enriched in our study, such as
236 ABC transporter and sulfur relay system. The DEGs involved in ABC transporters
237 (ABCA3, ABCB1, ABCC1, ABCG2, and PDR5) were shown in Figure 3H. In brief,
238 these results demonstrated that cell membrane, protein synthesis, functions related to
239 metabolism, and ribosome were significantly impacted by linalool and were potential
240 drug targets of linalool.

241 **2.4 The *in vivo* protective effect of linalool against *Saprolegniosis***

242 To study the protective effects of linalool on *S. parasitica* infection in fish, linalool
243 was added to grass carp after *S. parasitica* infection (linalool therapeutic group, LT) or
244 48 h before infection (linalool prophylactic group, LP), and a positive control group
245 (PC) without linalool and a negative control group (NC) without infection and linalool
246 were set up (Figure 4A). The results showed that the survival rate of *S. parasitica*
247 infected grass carp was significantly improved after treatment with linalool (Figure 4C),
248 which proved greatly anti-*Saprolegnia* activity of linalool. In Figure 4B, there was no
249 observable mycelium in both LT and LP groups, while the PC group displayed
250 significant mycelium growth along with inflammation on the dorsum. The LZM
251 activity was significantly increased in LP and LT group on the seventh day (Figure 4E),
252 yet the AKP activity (Figure 4D) was reduced. However, there was no significant
253 difference in the SOD activity (Figure 4F) between LP and LT groups during the whole
254 feeding trial.

255 To explore the histomorphology alterations caused by *S. parasitica* infection and
256 linalool treatment, we performed histomorphology evaluations through HE staining
257 (Figure 4G). The findings revealed significant pathological changes in the kidney, liver,
258 spleen, and skin of grass carp due to *S. parasitica* infection. In PC group, severe kidney
259 damage was evident, characterized by enlarged glomeruli, glomerular cysts, interstitial
260 bleeding, and infiltration of inflammatory cells. In addition, extensive vacuolation and

expansion of intercellular space was observed in hepatocytes, with nuclei displaced toward one side. Cytoplasmic pyknosis and structural disintegration were observed in the pancreatic acinar cells. Meanwhile, the red and white pulp of the spleen was poorly demarcated, the splenic corpuscle was irregularly shaped and arranged, and the white pulp was structurally disrupted. Furthermore, there was a notable increase in the number of macrophages and an expansion in the size of melanoma-macrophage centers. *S. parasitica* not only caused damage to both the dermal and epidermal layers but also induced muscle cell degeneration. Continuous treatment of linalool for 7 days significantly improved kidney, liver, spleen, and skin morphological integrity.

In the LP and LT groups, linalool alleviated tissue damage caused by *S. parasitica* infection on the dorsal surface of grass carp, enhancing the healing capacity (Figure 4B). Histomorphology demonstrated that linalool could improve the integrity of organ morphology in grass carp (Figure 4G). Transcriptomics of the spleen revealed that linalool promoted wound healing, tissue repair, and phagocytosis to cope with *S. parasitica* infection (Figure 5E). In all, our results indicated that linalool promoted wound healing in grass carp.

2.5 The *in vivo* Saprolegniasis protective mechanism of linalool revealed by comparative transcriptome analysis

To analyze the contrasting gene-level responses in grass carp spleens, a vital immune organ, following *S. parasitica* infection and linalool treatment, spleen samples were collected for transcriptome analysis. Compared to PC group, 2029 genes in LT group exhibited significant difference, with 809 DEGs up regulated and 1220 down regulated. Meanwhile, 671 genes were identified as significantly different, with 609 DEGs up-regulated and 618 downregulated in LP group relative to PC group (Figure S2A-B).

Based on the GO annotation analysis, a total of 2219 unigenes in the LT group and 520 unigenes in the LP group were classified into 3 primary functional categories (Figure S2C). Within the biological process category, "cellular process," "metabolic process," and "biological regulation" were the most prominent subcategories. In terms of cellular components, "membrane part" and "cell part" were highly represented.

"Binding" and "catalytic activity" were the most prevalent subcategories within molecular functions. Regarding KEGG annotations, the largest cluster within organismal systems was the immune system, encompassing 209 genes (42.47%) in the LT group (Figure S2D) and 38 genes (50.00%) in the LP group (Figure S2E). In the environmental information processing category, most unigenes were associated with signal transduction, with 227 (65.60%) in the LT group and 38 genes (52.00%) in the LP group. These results suggested that the immune response and signal transduction pathways were crucial for grass carp in dealing with *S. parasitica* infections.

The GO enrichment analysis of the spleens illustrated in Figure 5A-B to reveal distinct biological process. Those down regulated biological process were shown in Figure 5A, compared to PC group, the “positive regulation of immune system process” term (GO:0002684) and “regulation of body fluid levels” term (GO:0050878) were enriched with the greatest number of DEGs in LT group. It is worth noting that there are 9 terms related to "body fluids (especially blood)", such as regulation of coagulation (GO:0050818), blood coagulation (GO:0007596), and regulation of hemostasis (GO:1900046). In addition, those up regulated biological process, the “ion binding” term (GO:0043167) was enriched with the greatest number of DEGs in LT group. Figure 5B illustrated the GO terms with the largest number of down regulated DEGs in LP group was “small molecule binding” (GO:0036094).

KEGG enrichment analysis was used to explore the functional pathways involving DEGs. The 20 significantly enriched up regulated and down regulated pathways of each group are shown in Figure 5C-D. Multiple pathways associated with immune response were enriched in down regulated genes after linalool treatment in LT group, including complement and coagulation cascades, Toll-like receptor signaling pathway, IL-17 signaling pathway, C-type lectin receptor signaling pathway, T cell receptor signaling pathway, B cell receptor signaling pathway, and so on (Figure 5C). Toll-like receptor signaling pathway, RIG-I-like receptor signaling pathway, Complement and coagulation cascades, and Chemokine signaling pathway were enriched with mostly up-regulated genes. Furthermore, metabolic pathways were enriched with mostly

down-regulated genes in LP group. Some pathways associated with immune response were significantly enriched, such as Antigen processing and presentation, Fc epsilon RI signaling pathway, Intestinal immune network for IgA production, and so on (Figure 5D). GO and KEGG enrichment analyses revealed the presence of numerous immune-related genes within corresponding functional processes and pathways. The expression of *fb*, *c1q*, *c2*, *c3*, *c4*, *c6*, *c7*, *c8A*, *c8b*, and *c9* genes were up expressed. Additionally, there was a significant up expressed in the gene expression levels of coagulation factors II (thrombin), VII, VIIi, VIII, X, coagulation factor IXb and IXa, serpin peptidase inhibitor clade C/D/G/F, *fga*, *fgb*, *fgg*, protein C, plasminogen, and plasminogen activator (Figure 5E). The differential expression of immune-related DEGs implied their role in host defense against *S. parasitica* infection.

To ensure the regulation of immune-related DEGs by linalool, the expression of several vital immune related genes (*cfh*, *masp2*, *c1r*, *c3*, *cfb*, *ap-1*, *il-1β*, and *il-6*) in different groups were tested by RT-qPCR assay. The results showed that the expression of these genes in the LP and LT groups significantly exceeded those in the PC group ($P < 0.05$) (Figure 5H). Further exploration of immune-related genes indicated that linalool treatment promoted the expression of genes linked to the complement system and inflammatory factors. Additionally, analysis of 8 genes revealed that the real-time fluorescence quantitative analysis results were consistent with the expression trend of transcriptome analysis genes.

2.6 Linalool regulated gut microbiota composition

In our study, we explored the link between linalool and gut microbiota by conducting 16S sequencing analysis on 12 samples, which identified 862 OTUs in total, including 48 common OTUs shared across all samples. (Figure 6E). Alpha diversity analysis (Figure 6A-D) showed that the Simpson, Shannon, Chao1, and Ace index of gut microbiota decreased after linalool treatment which indicated that linalool reduced the abundance and diversity of gut microbes. The goal of PCoA is to preserve the distance relationships between samples as much as possible through the principal coordinates, thereby revealing the differences or patterns in microbial composition among different

348 groups. PCoA analysis showed a significant difference in microbial composition among
349 the positive control (PC), linalool prophylactic (LP), and linalool therapeutic (LT)
350 groups (Figure 6F).

351 The composition of gut microbiota in Figure 6G showed that the main dominant
352 bacteria in the intestinal tract are Proteobacteria, Actinobacteriota, Verrucomicrobiota,
353 Firmicutes, and Bacteroidota at the phylum level. Among them, compared with PC
354 group, an obvious tendency of greater relative abundances of phyla Proteobacteria and
355 Actinobacteriota was evidenced in linalool prophylactic (LP) and linalool therapeutic
356 (LT) groups, the relative abundance of Verrucomicrobiota was decreased. From the
357 composition of the genus level, the *Neochlamydia* decreased, while *Achromobacter*
358 increased. It is worth noting that the genus *Aurantimicrobium* (classified as
359 Actinobacteriota) was increased in linalool prophylactic (LP) and linalool therapeutic
360 (LT) groups. Notably, among biomarkers with an LDA SCORE exceeding 3, the genus
361 *Actinomycetales* bacterium held the highest number of positions, which contributed to
362 the major differences between the positive control and linalool treatment groups.
363 Moreover, the potential metabolic pathways of gut microbiota primarily showed
364 enrichment in functions related to metabolism, including carbohydrate, amino acid, and
365 cofactors and vitamins metabolism (Figure 6I).

366 **2.7 Correlation analysis of potential related immune genes, specific microbial**
367 **species, and physical characteristics**

368 Correlation analysis showed that complement system were significantly positively
369 correlated to Actinobacteriota, AKP, and SR (survival rate), which, in turn, a
370 significantly negatively correlated with Verrucomicrobiota. Additionally, there was a
371 significant positive correlation between PPRs and AKP. Notably, IgA related immune
372 genes were correlated significantly with Proteobacteria (Figure 6J). In summary, our
373 findings suggested that linalool effectively modulated gut microbiota during *S.*
374 *parasitica* infection which was associated with immune response.

375 **3. Discussion**

376 **3.1 *In vitro* mode of action of linalool against *S. parasitica***

3.1.1 Membrane disruption

The cell membrane maintains cell integrity, regulates substance entry and exit, while the cell wall provides structural support, protection, and promotes growth and cell-to-cell connections[32]. The mycelium forms a dense structure to protect *S. parasitica* spores from external factors. CLSM, SEM, and TEM observations suggested that the cell membrane of the mycelium treated with linalool was damaged, causing the intracellular components to leak out, and could not develop completely (Figure 2A-G). Meanwhile, 678 genes related to the "intrinsic component of membrane" showed significant expressed in GO enrichment analysis, suggesting that linalool may enhance the expression of intracellular membrane components, reflecting its impact on cell membrane structure or function. Gao et al. illustrated that linalool caused significant damage to the cell wall/membrane of *E. coli*, resulting in the lysis and death of bacterial cells[12]. Gao et al. demonstrated that linalool[17], *Changshan-huyou* Y.B. Chang EO[33], and Fingered Citron EO[34] can disrupt the cell membrane of *L. monocytogenes*. Lemon essential oil nanoemulsions altered the permeability of *E. coli* cell membrane, affecting membrane potential, integrity, and efflux function[35]. Cruz et al suggested that alkamides in *Echinacea* disrupted the cell wall/membrane complex, making it an ideal target for specifically inhibiting pathogens[36]. Hinokitiol caused mycelium malformation by inducing cell component leakage and influencing chitinase activity[37]. Therefore, linalool may act anti-oomycete effects against *S. parasitica* by targeting the cell membrane.

ABC transporters utilize ATP hydrolysis energy to facilitate the export of harmful compounds or essential lipids across bacterial and eukaryotic membranes[38]. The DEGs involved in ABC transporters (ABCA3, ABCB1, ABCC1, ABCG2, and PDR5) in our study, almost all of which have been linked to illness states usually involving loss of function[39]. PDR5-related proteins in fungi played a role in excreting xenobiotics, including antifungal agents[40]. Multidrug resistance-associated protein (MRP) transporters were typically associated with multidrug resistance, cellular detoxification, and drug metabolism[41]. To sum up, linalool may greatly inhibit mycelium growth by

interfering with protein synthesis from the "inside" and damaging the integrity and permeability of the cell membrane and wall from the "outside."

3.1.2 Reduction of ribosome biogenesis and RNA polymerase

To further investigate the mechanism of linalool against *S. parasitica*, the gene expression profiles of *S. parasitica* were compared (with or without exposed to linalool). Many DEGs related to ribosome biogenesis and RNA polymerase were down expressed, indicating that the linalool may influence translation, replication, and repair processes, leading to increased protein diversity and potential disruption of corresponding functions[42]. Linalool influenced DNA transcription, tRNA transport, rRNA processing and maturation (5.8S, 18S, and 25S), and the biogenesis and assembly of ribosome subunits (40S and 60S) in the cell, which might lead to the reduction of *S. parasitica* growth. Ribosomes are assembled logistically by more than 200 ribosomal proteins (such as NOP, RIOK, and UTP) and RNA factors in a highly coordinated manner[43]. Depletion of Nop-7-associated 2 (NSA2) led to decreased nascent rRNA synthesis, reduced protein synthesis, and impacted cell proliferation due to its critical role in ribosome biogenesis regulation[44]. The inhibitory effect of myriocin on *Fusarium oxysporum* includes both membrane damage and interactions with intracellular targets, such as proteins like RIOK2, within the ribosome biogenesis pathway[45]. Innate immunity in *Caenorhabditis elegans* has been discovered to be negatively regulated by NOL-6 (also named UTP22)[46]. The growth of *Aspergillus niger* may be inhibited by cyclosporin A because it may prevent the transcription and translation of the RNA polymerase III complex[47]. Rifampicin can prevent RNA transcription in bacteria by interacting with the β-subunit of DNA-dependent RNA polymerase, which can then inhibit protein biosynthesis[48]. These results indicated that the down-regulation genes may limit the proteins necessary for normal cell biogenesis and growth. Therefore, ribosome is a promising potential target of linalool against *S. parasitica*.

3.1.3 The influence on the metabolism function of *S. parasitica*

Metabolism function is crucial for cells to maintain homeostasis, survive, and proliferate[49]. Linalool caused the activation of energy metabolism pathways,

435 compensating for the insufficient energy needed for cell survival[50]. In our study,
436 linalool was found to enhance amino acid metabolism, carbohydrate metabolism,
437 energy metabolism, and so on in mycelial cells, which suggested that cells may boost
438 functions related to energy metabolism to acquire additional energy for repairing
439 damage caused by linalool. Hence, linalool treatment caused intracellular energy
440 metabolism disruption, resulting in impediments to protein synthesis, cellular signal
441 transduction, DNA synthesis, and ultimately affecting cell viability and proliferation.

442 **3.1.4 The difference *in vitro* mechanisms between *S. parasitica* and *S. ferax***

443 In our previous study, we found that linalool affected *S. ferax* mainly by altering
444 membrane permeability, causing permanent damage, and membrane breakdown;
445 affecting the oxidation and metabolism of fatty acids and lead to mitochondrial
446 dysfunction and the inhibition of energy supply; degrading the branched chain amino
447 acids and result in the dysfunction of protein synthesis. While, for *S. parasitica*, linalool
448 exhibited antimicrobial activity by prohibiting ribosome function, inhibiting protein
449 synthesis, disrupting the cell membrane of the mycelium. We found several interesting
450 phenomena when compared these two species. Firstly, the inhibition of protein
451 synthesis was found in both species, but the interesting difference is that linalool
452 inhibits protein synthesis through degrading the branched chain amino acids in *S. ferax*,
453 while through prohibited ribosome function in *S. parasitica*. Secondly, linalool affected
454 the oxidation and metabolism of fatty acids and mitochondrial dysfunction in *S. ferax*,
455 while not found in in *S. parasitica*. These phenomena showing above are very
456 interesting results and we are eager to explore the biological mechanisms in the future.

457 **3.2 *In vivo* mode of action of linalool against *S. parasitica* infection**

458 Recent studies demonstrated that the spleen serves antibacterial functions in various
459 fish species, with a high quantity of melano-macrophages that assist in phagocytosis
460 during the immune response[51]. The rise of macrophages and the change in the
461 pathological and physiological circumstances in fish are correlated[52]. Similarly,
462 histopathological analysis demonstrated that linalool effectively reduced *S. parasitica*
463 infection-induced damage in the spleen, indicating its potential immunomodulatory

effects on immune organs. Here we used comparative transcriptome analysis to investigate potential genes and signaling pathways regulated by linalool in the spleen of grass carp. Several genes associated with both innate and adaptive immunity, such as complement molecules, pattern recognition receptors, inflammatory cytokines, immunoglobulins, and chemokines, were differentially expressed as shown in Figure 5E-G.

3.2.1 Enhancement of complement and coagulation system

It is widely acknowledged that the complement and coagulation system in fish is an important immune defense mechanism for fighting pathogens and maintaining immune homeostasis[53]. The complement system is made up of over 30 different proteins (complement receptors, internal components, and regulatory proteins) and 3 activation pathways (the classic pathway, the lectin pathway, and the alternative pathway)[54]. In our study, the expression of *fb*, *c1q*, *c2*, *c3*, *c4*, *c6*, *c7*, *c8a*, *c8b*, and *c9* genes were all up regulated after linalool therapeutic. Meanwhile, the c3a anaphylatoxin chemotactic receptor (*c3aar1*) and mannan-binding lectin serine protease 2 (*masp2*) genes were up expressed. During complement activation, *c3* and *c5* split into molecules such as *c3a*, *c3b*, *c5a*, and *c5b*, of which *c3a* and *c5a* are considered strong inflammatory mediators because of their ability to attract leukocytes and promote inflammation and pathogen clearance[55]. *masp2* activates complement components such as *c4* and *c2*, triggering a complement cascade reaction that ultimately leads to pathogen rupture[56]. *c8b* is a subunit of the complement component 8 (*c8*) protein, which helps form the membrane attack complex (MAC) for cell lysis and immune defense against microbes[57]. In addition, high expression of complement factor H like 3 (*chfl3*) prevents overactivation of the complement system to avoid damage to their own tissues[58]. The effective antimicrobial role of the *c5a-c5ar1* signaling pathway in the complement system has been identified. It functions by enhancing neutrophil phagocytosis of fungi and macrophage-mediated fungicidal activity to combat fungal infections[59]. In all, our findings suggested that linalool may enhance the complement system which in turn activated host immune defense and lysate *S. parasitica* cells.

The coagulation cascades are connected with the complement system. Linalool significantly increased the expression of fibrinogen alpha (*fga*), beta (*fgb*), and gamma (*fgg*) chain, which together encoded fibrinogen[60], fibrinogen is a crucial component of blood clots to prevent blood loss, and also important in the initial stages of wound healing[61]. Secondly, activated prothrombin *f2* is central in clot formation, platelet aggregation, and activating other clotting factors. It also supports tissue repair, cell growth, angiogenesis, and vascular integrity[57]. Thirdly, an increase in plasminogen (PLG) levels can cause an immune response[62], and serve as a regulator of the natural immune system by promoting the phagocytosis of phagocytes[63]. Taken together, the upregulation of fibrinogen, prothrombin, and plasminogen in the coagulation system suggested that linalool may promote wound healing, tissue repair, and phagocytosis to cope with *S. parasitica* infection.

3.2.2 Regulation of gut microbiota and increase the abundance of Actinobacteriota

Gut microbiota controls host growth and health status through various pathways[64]. Firstly, in our study, the function of gut microbiota is mainly enriched in metabolic-related pathways linalool increased the abundance of the beneficial phylum Actinobacteriota and decreased the abundance of the harmful phylum Verrucomicrobiota. Actinobacteriota plays a crucial role because Actinobacteria can produce enzymes, antibiotics, Short-chain fatty acids (SCFAs), signaling molecules, and immunomodulators[65]. Meanwhile, Actinobacteriota correlated positive with the complement and coagulation system according to the correlation analysis. Secondly, intestinal IgA production was correlated significantly with Proteobacteria which are the primary inducers of IgA production by B cells[66]. In summary, our findings suggested that linalool may positively modulate the immune response by increasing the abundance of beneficial phylum Actinobacteriota to *S. parasitica* infection.

3.2.3 Regulation of Inflammatory Factors

Pattern Recognition Receptors (PPRs) detect and initiate multiple signaling pathways upon recognizing Pathogen-Associated Molecular Patterns (PAMPs) on the surface of pathogens (bacteria, viruses, fungi, etc.), inducing subsequent host immune

responses[67]. Myeloid differentiation primary-response protein 88 (MyD88) serves as the crucial signaling adaptor protein for Toll-like and interleukin-1 receptors, which is responsible for the conduction of multiple downstream signaling pathways[68]. The expression of *ap-1*, *p-38*, and *pI3k* were up regulate in downstream signaling pathways, causing higher expression of inflammatory factors, and enhanced cellular oxidation and antioxidant levels[69]. Meanwhile, in our study, the gene expression levels of *il-1β*, *il-6*, *ccl19*, and *ccl5* which are closely related to the inflammasome, were up expression. Inflammasomes are protein complexes capable of detecting diverse inflammatory stimuli and are vital for eliminating pathogens or injured cells[70]. Therefore, linalool might have influenced the immune system response in grass carp, regulating the inflammatory processes.

4. Conclusions

In summary, our study proved that linalool is an effective natural antimicrobial agent against *S. parasitica*. Linalool disrupted the cell membrane, resulting in the leakage of cellular components and restricting ribosomal function, thereby inhibiting protein synthesis. Comprehensive analyses revealed the specific role of linalool in protecting *S. parasitica* infection skin inflammation in grass carp. Meanwhile, the complement and coagulation systems, inflammatory factors, along with Actinobacteriota, significantly involved in this protective effect (Figure 7). Further investigation would be carried out to explore and refine how linalool affects the inflammatory effects of *S. parasitica* on fish through signaling pathways and mechanisms. We believe that this study will contribute to developing an innovative alternative strategy, distinct from antibiotics, to cope with *S. parasitica* infection in the aquaculture industry.

5. Materials and methods

5.1 Oomycete strains and materials

S. parasitica used in this study was from our lab, which was isolated from grass carp (*Ctenopharyngodon idella*). Linalool (0.862g/mL), pinene (0.874g/mL), limonene (0.842g/mL), myrcene (≥95%), terpinene (≥95%), resazurin dye, and Prodium iodide (PI) were purchased from Sigma-Aldrich (USA). SYTO 9 and FM4-64 were purchased

from ThermoFisher (USA). Potato dextrose agar (PDA) and glucose yeast extract (GY) were purchased from Guangdong Huankai Microbial Sci. and Tech. Co., Ltd, China.

5.2 Agar diffusion assay

The anti-oomycetes effects of EOs and 5 components (linalool, terpinene, limonene, myrcene, and pinene) were assessed by using the agar diffusion method. Initially, a 6 mm mycelium plug was inoculated at the center of the plates. Subsequently, 6 mm sterile filter paper discs were soaked in EOs and components for more than 12 h and placed symmetrically at a distance of 2.5 cm from the target mycelium plug. Sterile distilled water was used as negative control. Finally, the width of the colonies was measured once the mycelium in the control group was completely covered the plate.

Inhibition rate (%) = [(P1 − P2)/P1] × 100%, where, P1 = colony growth diameter (mm) of control group, P2 = colony growth diameter (mm) of treated group.

5.3 Minimum inhibitory concentration (MIC) and minimum fungicidal concentration (MFC) assays.

To determine the MIC and MFC of linalool on mycelium, 6 mm mycelium plugs were inoculated into a 24 well cell culture plate. The wells contained linalool at concentrations of 0.8%, 0.4%, 0.2%, 0.1%, 0.05%, 0.025%, 0.0125%, and 0.00625%, dissolved in 1% Tween 20 and potato dextrose broth (PDB). Wells without mycelium plugs were served as negative controls. After incubating at 25°C for 48 h, the lowest concentration of linalool with no visible mycelium growth was recorded as MIC. Mycelium plugs showing no growth at this MIC concentration then inoculated onto PDA plates and incubated for 7 days at 25°C to determine MFC.

The method for spores induction is similar as previously described by our previous research[15]. In a 96-well cell culture plate, 100 μL of linalool at concentrations of 0.4%, 0.2%, 0.1%, 0.05%, 0.025%, 0.0125%, 0.00625%, and 0.003125% were dissolved in 1% Tween 20 and GY were added initially to each well, followed by the addition of 100 μL of spore suspension at a concentration of 1×10^6 spores/mL to each well. 2.5 mg/mL malachite green and 1% Tween 20 served as positive and negative controls, respectively. Following a 24-hour incubation at 20°C, 5 μL of resazurin dye was added.

When the color of the wells turned to pink, the linalool concentration in the first non-pink well corresponded to the MIC. The culture liquid from wells with no visible mycelium growth was streaked onto new plates. After incubating at 25°C for 7 days, the well with the lowest linalool concentration with no visible mycelium growth was determined as MFC.

5.4 Effect of linalool on the mycelium radial growth rate of *S. parasitica*

Different concentrations of linalool were added to molten PDA plates at 50°C for quantitative assessment. A similarly sized mycelium plug was placed at the center of each plate. Once the mycelium in the control group without linalool reached the edge of the plate (approximately 60 h), the radial diameter of the mycelium was measured. The calculation of growth inhibition was determined by assessing the percentage inhibition of radial growth, as below:

The percentage inhibition of radial growth (PIRG %) = [(R1− R2)/R1] × 100%, where, R1 = radial growth of control plate (mm), R2 = radial growth of treatment plate (mm)

5.5 Confocal laser scanning microscopy (CLSM) assay

2.5.1 Analysis of viability of *S. parasitica*

The mycelium was treated with linalool at MIC (0.05%) and 2×MIC (0.1%) for 2 h, and untreated control group was prepared simultaneously. The mycelium resuspended in PBS was further treated with PI at a final concentration of 2.5 g/mL for 15 minutes. PI is excited at a wavelength of 488 nm and emits light at 620 nm. Fluorescence images were observed using CLSM (LSM880, Zeiss, Germany) at 40× magnification.

2.5.2 Analysis of membrane damage of *S. parasitica*

Mycelium cultured for 18 h was collected and sequentially treated with SYTO 9 at a concentration of 20 μmol/mL, FM4-64 at a concentration of 10 μmol/mL, and linalool at a concentration of 3%. Record observations at 0, 2, 8, and 20 min. Both SYTO 9 and FM4-64 have an excitation wavelength of 488 nm and emit light at 620 nm and 520 nm, respectively. Fluorescence images were observed using CLSM (LSM880, Zeiss, Germany) at 40× magnification.

609 **5.6 Scanning Electron Microscope (SEM) assay and transmission electron**
610 **microscopy (TEM) assay**

611 Mycelium exposed to MIC (0.05%) linalool for 2 h underwent fixation with 2.5%
612 glutaraldehyde at 4°C for 4 h to examine the impact of linalool on membrane damage.
613 Following a rinse with phosphate-buffered saline (PBS; pH 7.2), the fixed samples
614 experienced dehydration for 15 min using a graded series of ethanol concentrations
615 (10%, 30%, 50%, 70%, 90%, and 100%), followed by an additional 20 min in 100%
616 ethanol. Post-dehydration, ethanol was exchanged twice for 20 min each with tertiary
617 butanol. Subsequently, the samples were subjected to vacuum freeze-drying, gold-
618 spraying, and examination with SEM (Hitachi, SU8010). After fixation, the samples
619 were ultrathin-sectioned, subjected to negative staining using 1% phosphotungstic acid
620 for 5 min and observed by TEM (Hitachi, HT-7700).

621 **5.7 RNA-Seq and bioinformatics analysis**

622 Total RNA was isolated from linalool treated (exposed to 0.5×MIC linalool for 10
623 minutes) and untreated control groups using the TRIzol method. The messenger RNA
624 (mRNA) was enriched and fragmented into 200 bp fragments. These mRNA fragments
625 were reverse-transcribed into cDNA using random primers and reverse transcriptase.
626 The cDNA ends were modified and ligated to an adaptor. After PCR amplification and
627 purification, Illumina sequencing was performed. Quality control removed low-quality
628 reads. The mapped reads were assembled using StringTie. Gene expression was
629 quantified with the transcripts-per-million-reads method to identify differentially
630 expressed genes (DEGs) using a threshold of |log twofold change| ≥ 2 and FDR < 0.05.
631 Afterward, functional enrichment analysis was performed using the Kyoto
632 Encyclopedia of Genes and Genomes (KEGG) database. KEGG pathway analysis was
633 conducted using Goatools. The Majorbio cloud platform was used for data analysis[71].

634 **5.8 Molecular docking**

635 Linalool may interact with specific domains of the ribosome, potentially influencing
636 its structure and function. Therefore, our investigation aimed to determine whether
637 linalool could bind to the ribosome-associated upstream proteins of *S. parasitica*. As

no crystal structure of *S. parasitica* ribosome proteins existed in the Protein Data Bank (PDB), we performed homology modeling. The protein sequences NOP1 (XP_012204452.1), SNU13 (XP_012198008.1), and DKC1 (XP_012193765.1) were obtained from GenBank, and homology modeling was conducted using AlphaFold2. The most optimal configuration identified from the homologous modeling results was chosen as the receptor protein for subsequent molecular docking. The model was then evaluated using ProSA-web and PROCHECK server. The secondary structure of linalool was then loaded on PubChem. Both the ligand (linalool) and target proteins underwent processing with AutoDockTools 1.5.6, including energy minimization, dehydration, and hydrogenation. The conformation exhibiting the lowest energy was selected as the most likely binding state. The ultimate docking outcome was visualized utilizing the open-source software PyMOLv2 and Discovery Studio Visualizer V2021.

5.9 Animal Experiments

5.9.1 Ethics statement

All experiments involving animals were conducted according to the ethical policies and procedures approved by the Institutional Animal Care and Use Committee of Hunan Agricultural University, China (Approval No. 430516).

5.9.2 Linalool therapeutic and prophylactic assays

In this study, 4 groups were established: (1) Positive control (PC) group (10 fish infected with *S. parasitica*). (2) Linalool therapeutic (LT) group (10 fish infected with *S. parasitica*, soaked in 0.00039% linalool in a 20L tank for 7 days). (3) Linalool prophylactic (LP) group (10 uninfected fish soaked in 0.00039% linalool in a 20L tank for 2 days, followed by the addition of 1×10^6 spores/mL secondary zoospores). (4) Negative control (NC) group (10 uninfected fish without linalool treatment). Each group had 3 replicate tanks. The number of fish without visible mycelium on day 7 and the cumulative survival rate were recorded. The fish samples from the negative control (NC), positive control (PC), linalool therapeutic (LT), and linalool prophylactic (LP) groups were collected for histopathological examinations. Tissue samples underwent

666 fixation, sectioning, hematoxylin and eosin (H&E) staining, and microscopic
667 examination using a microscope (BX53, Olympus).
668 5.9.3 16S rRNA and transcriptome sequencing and analysis
669 Genomic DNA was extracted from grass carp intestinal content samples and stored
670 at -20°C following the instructions of the 16S rRNA gene pyrosequencing DNA kit. We
671 conducted paired-end sequencing on the Illumina MiSeq platform, amplifying the V3-
672 V4 regions with specific barcoded primers using a thermocycler PCR system. To unveil
673 the intricate microbial diversity within the samples, we employed Quantitative Insights
674 Into Microbial Ecology (QIIME) which can compute and visualize α-diversity, β-
675 diversity, and principal coordinate analysis (PCoA). α-diversity measured the species
676 richness and evenness within a single sample, reflecting the complexity of the
677 community; β-diversity compared the differences in species composition between
678 samples, revealing changes in community structure; Principal Coordinate Analysis
679 (PCoA), based on a distance matrix, visualized the differences between samples,
680 providing an intuitive display of community clustering and distribution. Each sample
681 was measured 3 times to ensure robust results.
682 Spleen tissue was obtained from 3 fish in each group on day 7. These collected spleen
683 tissues were promptly flash-frozen in liquid nitrogen and then stored at -80°C until they
684 were ready for RNA isolation. RNA-Seq and bioinformatics analysis was carried out as
685 shown in Section 2.6.
686 In each group, 8 fish were utilized for immunological assays, and on day 7, blood
687 samples were collected from the tail veins using heparinized syringes and left to
688 coagulate overnight at 4°C. After centrifugation at 3500×g for 10 minutes at 4°C, serum
689 was obtained from each fish and stored at -80°C for subsequent analysis. Kits from
690 Nanjing Jiancheng Institute (Nanjing, China) were used to measure lysozyme (LZY)
691 activity, superoxide dismutase (SOD) activity, and alkaline phosphatase (AKP) activity.
692 **5.10 Detection of immune-related gene expression**
693 Spleen tissues RNA extraction utilized the EZNA Total RNA Kit II (OMEGA R6934-
694 02). RNA concentrations were quantified using a spectrophotometer (Eppendorf

BioSpectrometer basic, Germany), and quality assessment was conducted through 1% gel electrophoresis. Subsequent cDNA synthesis employed reverse transcription with the RevertAid First Strand cDNA Synthesis Kit (Thermo Fisher Scientific, USA). RNA concentrations were quantified via spectrophotometry (Eppendorf BioSpectrometer basic, Germany). Subsequently, cDNA was synthesized via reverse transcription using the RevertAid First Strand cDNA Synthesis Kit (Thermo Fisher Scientific, USA). Expression levels of complement factor H (*cfh*), mannan-binding lectin serine protease 2 (*masp2*), complement component 1, r subcomponent (*c1r*), complement component 3 (*c3*), complement factor B (*cfb*), transcription factor AP-1 (*ap-1*), interleukin 1 beta (*il-1β*) and interleukin 6 (*il-6*) were detected. The PCR procedure was described as follows: 95 °C for 30 s, followed by 40 cycles of 95 °C for 5 s and 60 °C for 40 s. Employing the CFX96 Touch Real-time PCR Detection System (Bio-rad, USA), gene expression levels were assessed using the $2^{-\Delta\Delta Ct}$ method, with β-actin serving as the reference gene. The primers in qPCR analysis are listed in Table 1.

5.11 Statistical analysis

The data was expressed as mean ± standard error, and all experiments were conducted in triplicate. Pearson correlation analysis was employed to investigate the correlation between potential immune-related genes in grass carp and their characteristics, the method was implemented in R Programming language. Statistical analysis was performed using GraphPad Prism 9 software, and the student t-test was conducted.

Acknowledgments

This research was funded by National Natural Science Foundation of China (32073020, 32201960), Science and Technology Innovation Program of Hunan Province (2022RC1150), Hunan Provincial Natural Science Foundation of China (2023JJ40364), and Agricultural Science and Technology Innovation Fund of Hunan (2023CX49).

Author contributions

Tao Tang was in charge of conceptualization, methodology, writing-original draft, writing-review & editing.

Weiming Zhong was in charge of data curation.

Puyu Tang was in charge of methodology.

Rongsi Dai was in charge of data curation.

Jiajing Guo was in charge of writing - review & editing.

Zhipeng Gao was in charge of funding acquisition, supervision, writing-original draft, writing-review & editing.

Declaration of interests

The authors declare no competing interests.

Data and code availability

The data that support the findings of this study are available in the supplementary material of this article and are available from the corresponding author upon reasonable request.

References

[1] Derevnina, L., Petre, B., Kellner, R., et al. 2016. Emerging Oomycete Threats to Plants and Animals. Philosophical Transactions of the Royal Society B-Biological Sciences 371, 9 20150459. https://doi.org/10.1098/rstb.2015.0459.

[2] Tandel, R. S., Chadha, N. K., Dash, P., et al. 2021. An *in Vitro* Study of Himalayan Plant Extracts against Oomycetes Disease Saprolegniasis in Rainbow Trout (*Oncorhynchus Mykiss*). Journal of Environmental Biology 42, 1008-18. https://doi.org/10.22438/jeb/42/4/MRN-1623.

[3] Wang, H. Z., Li, D. L., Fan, M. H., et al. 2021. Identification and Expression Analysis of Ricin B-Like Lectin Genes in the Fish Pathogen *Saprolegnia Parasitica*. Aquaculture International 29, 1853-68. https://doi.org/10.1007/s10499-021-00722-5.

[4] Costa, S., and Lopes, I. 2022. Saprolegniosis in Amphibians: An Integrated Overview of a Fluffy Killer Disease. Journal of Fungi 8, 30 537. https://doi.org/10.3390/jof8050537.

[5] Sandoval-Sierra, J. V., Latif-Eugenin, F., Martín, M. P., et al. 2014. *Saprolegnia* Species Affecting the Salmonid Aquaculture in Chile and Their Associations with Fish Developmental Stage. Aquaculture 434, 462-69. https://doi.org/10.1016/j.aquaculture.2014.09.005.

[6] Khulbe, R. D., Joshi, C., and Bisht, G. S. 1995. Fungal Diseases of Fish in Nanak Sagar, Naini Tal, India. Mycopathologia 130, 71-4. https://doi.org/10.1007/bf01103452.

[7] Engblom, C., Landor, L., Sjöqvist, C., et al. 2023. Identification and Genetic Characterization of *Saprolegnia Parasitica*, Isolated from Farmed and Wild Fish in Finland. Journal of Fish Diseases 46, 849-60. https://doi.org/10.1111/jfd.13795.

[8] Money, N. P., Davis, C. M., and Ravishankar, J. P. 2004. Biomechanical Evidence for Convergent Evolution of the Invasive Growth Process among Fungi and Oomycete Water Molds. Fungal Genetics and Biology 41, 872-76. https://doi.org/10.1016/j.fgb.2004.06.001.

[9] Van West, Pieter. 2006. *Saprolegnia Parasitica*, an Oomycete Pathogen with a Fishy Appetite:: New Challenges for an Old Problem. Mycologist 20, 99-104. https://doi.org/10.1016/j.mycol.2006.06.004.

[10] van den Berg, A. H., McLaggan, D., Diéguez-Uribeond, J., et al. 2013. The Impact of the Water Moulds *Saprolegnia Diclina* and *Saprolegnia Parasitica* on Natural Ecosystems and the Aquaculture Industry. Fungal Biology Reviews 27, 33-42. https://doi.org/10.1016/j.fbr.2013.05.001.

[11] Yu, J. J., Hu, Y. L., Liu, C. Z., et al. 2023. Arscp: An Antimicrobial Residue Surveillance Cloud Platform for Animal-Derived Foods. Science of the Total Environment 858, 7 159807. https://doi.org/10.1016/j.scitotenv.2022.159807.

[12] Gao, Zhipeng, Jiang, Sifan, Zhong, Weiming, et al. 2023. Linalool Controls the Viability of *Escherichia Coli* by Regulating the Synthesis and Modification of Lipopolysaccharide, the Assembly of Ribosome, and the Expression of Substrate Transporting Proteins. Food Research International 164, 112337.

[13] Liu, Y. H., Espinosa, C. D., Abelilla, J. J., et al. 2018. Non-Antibiotic Feed Additives in Diets for Pigs: A Review. Animal Nutrition 4, 113-25. https://doi.org/10.1016/j.aninu.2018.01.007.

[14] Shehata, A. A., Yalçin, S., Latorre, J. D., et al. 2022. Probiotics, Prebiotics, and Phytogenic Substances for Optimizing Gut Health in Poultry. Microorganisms 10, 34 395. https://doi.org/10.3390/microorganisms10020395.

[15] Tang, Tao, Zhong, Weiming, Yang, Linlin, et al. 2023. *In Vitro* and *in Vivo* Anti-Oomycetes Activities and Mechanisms of Linalool against *Saprolegnia Ferax*. Aquaculture, 740031.

[16] Peana, A. T., D'Aquila, P. S., Panin, F., et al. 2002. Anti-Inflammatory Activity of Linalool and Linalyl Acetate Constituents of Essential Oils. Phytomedicine 9, 721-26. https://doi.org/10.1078/094471102321621322.

[17] Zhipeng, Gao, Weiming, Zhong, Ting, Liu, et al. 2021. Global Proteomic Analysis of *Listeria Monocytogenes'* Response to Linalool. Foods 10, 2449. https://doi.org/10.3390/foods10102449.

[18] Praseetha, S., Sukumaran, S. T., Dan, M. T., et al. 2023. The Anti-Biofilm Potential of Linalool, a Major Compound from *Hedychium Larsenii*, against *Streptococcus Pyogenes* and Its Toxicity Assessment in *Danio Rerio*. Antibiotics-Basel 12, 18 545. https://doi.org/10.3390/antibiotics12030545.

[19] Li, Y. S., He, R. R., Chen, H. M., et al. 2022. Respiratory Depression as Antibacterial Mechanism of Linalool against *Pseudomonas Fragi* Based on Metabolomics. International Journal of Molecular Sciences 23, 13 11586. https://doi.org/10.3390/ijms231911586.

[20] Aytac, Z., Yildiz, Z. I., Kayaci-Senirmak, F., et al. 2017. Electrospinning of Cyclodextrin/Linalool-Inclusion Complex Nanofibers: Fast-Dissolving Nanofibrous Web with Prolonged Release and Antibacterial Activity. Food Chemistry 231, 192-201. https://doi.org/10.1016/j.foodchem.2017.03.113.

[21] Rongrong, He, Qiuping, Zhong, Weijun, Chen, et al. 2022. Antimicrobial Mechanism of Linalool against *Brochothrix Thermosphacta* and Its Application on Chilled Beef. Food Research International 157, 111407. https://doi.org/10.1016/j.foodres.2022.111407.

[22] Zhong, W. M., Tang, P. Y., Liu, T., et al. 2021. Linalool Nanoemulsion Preparation, Characterization and Antimicrobial Activity against *Aeromonas Hydrophila*. International Journal of Molecular Sciences 22, 10 11003. https://doi.org/10.3390/ijms222011003.

[23] Jiang, Y., Pan, X. Y., Li, Y. M., et al. 2023. Linalool Induces Resistance against Tobacco Mosaic Virus in Tobacco Plants. Plant Disease 107, 2144-52. https://doi.org/10.1094/pdis-09-22-2246-re.

[24] Yang, J. J., Wang, Q. Z., Li, L. W., et al. 2022. Chemical Composition and Antifungal Activity of *Zanthoxylum Armatum* Fruit Essential Oil against *Phytophthora Capsici*. Molecules 27, 17 8636. https://doi.org/10.3390/molecules27238636.

[25] Li, Y. N., Zhang, S. B., Lv, Y. Y., et al. 2022. Linalool, the Main Volatile Constituent from *Zanthoxylum Schinifolium* Pericarp, Prevents Growth of *Aspergillus Flavus* in Post-Harvest Grains. Food Control 137, 13 108967. https://doi.org/10.1016/j.foodcont.2022.108967.

[26] Satoh, M., Kusumoto, N., Matsui, N., et al. 2022. Antitermitic and Antifungal Properties of Enantiopure Linalool and Furanoid Linalool Oxide Confirmed in *Lindera Umbellata* Var. *Membranacea*. Journal of Wood Chemistry and Technology 42, 37-45. https://doi.org/10.1080/02773813.2021.2004166.

[27] Gomes, P. R. B., Cunha, M. J. O., de Sousa, D. A., et al. 2019. Chemical Study and Antifungal Activity of the Essential Oil of the Branches of *Aniba Duckei* Kostermans. Journal of Essential Oil Bearing Plants 22, 1554-61. https://doi.org/10.1080/0972060x.2019.1700829.

[28] Shen, Q., Li, H. S., Wang, Q. F., et al. 2022. Alleviating Effects of Linalool Fumigation on *Botrytis Cinerea* Infections in Postharvest Tomato Fruits. Horticulturae 8, 15 1074. https://doi.org/10.3390/horticulturae8111074.

[29] Marcos-Arias, C., Eraso, E., Madariaga, L., et al. 2011. In Vitro Activities of Natural Products against Oral *Candida* Isolates from Denture Wearers. Bmc Complementary and Alternative Medicine 11, 7 119. https://doi.org/10.1186/1472-6882-11-119.

[30] Fischer-Parton, S., Parton, R. M., Hickey, P. C., et al. 2000. Confocal Microscopy of Fm4-64 as a Tool for Analysing Endocytosis and Vesicle Trafficking in Living Fungal Hyphae. Journal of Microscopy 198, 246-59. https://doi.org/10.1046/j.1365-2818.2000.00708.x.

[31] Yan, L. J., and Lamb, R. F. 2012. Amino Acid Sensing and Regulation of Mtorc1. Seminars in Cell & Developmental Biology 23, 621-25. https://doi.org/10.1016/j.semcdb.2012.02.001.

[32] Athanasopoulos, A., André, B., Sophianopoulou, V., et al. 2019. Fungal Plasma Membrane Domains. Fems Microbiology Reviews 43, 642-73. https://doi.org/10.1093/femsre/fuz022.

[33] Jiajing, Guo, Zhipeng, Gao, Gaoyang, Li, et al. 2019. Antimicrobial and Antibiofilm Efficacy and Mechanism of Essential Oil from Citrus Changshan-Huyou Y. B. Chang against *Listeria Monocytogenes*. Food Control 105, 256-64. https://doi.org/10.1016/j.foodcont.2019.06.014.

[34] Zhipeng, Gao, Weiming, Zhong, Kangyong, Chen, et al. 2020. Chemical Composition and Anti-Biofilm Activity of Essential Oil from *Citrus Medica* L. Var. *Sarcodactylis Swingle* against *Listeria Monocytogenes*. Industrial Crops and Products 144, 112036. https://doi.org/10.1016/j.indcrop.2019.112036.

[35] Wenbin, Xiao, Gao, Zhipeng, Liu, Ting, et al. 2023. Lemon Essential Oil Nanoemulsions: Potential Natural Inhibitors against *Escherichia Coli*. Food Microbiology, 104459.

[36] Cruz, I., Cheetham, J. J., Arnason, J. T., et al. 2014. Alkamides from *Echinacea* Disrupt the Fungal Cell Wall-Membrane Complex. Phytomedicine 21, 435-42. https://doi.org/10.1016/j.phymed.2013.10.025.

[37] Meng, F. Y., Liu, X., Li, C., et al. 2023. Hinokitiol Inhibits *Aspergillus Fumigatus* by Interfering with the Cell Membrane and Cell Wall. Frontiers in Microbiology 14, 11 1132042. https://doi.org/10.3389/fmicb.2023.1132042.

[38] Ford, R. C., and Beis, K. 2019. Learning the Abcs One at a Time: Structure and Mechanism of Abc Transporters. Biochemical Society Transactions 47, 23-36. https://doi.org/10.1042/bst20180147.

[39] Dean, M., Hamon, Y., and Chimini, G. 2001. The Human Atp-Binding Cassette (Abc) Transporter Superfamily. Journal of Lipid Research 42, 1007-17.

[40] van den Brule, Sybille, Muller, Axel, Fleming, Andrew J., et al. 2002. The Abc Transporter Sptur2 Confers Resistance to the Antifungal Diterpene Sclareol. The Plant journal : for cell and molecular biology 30, 649-62. https://doi.org/10.1046/j.1365-313X.2002.01321.x.

[41] Rees, D. C., Johnson, E., and Lewinson, O. 2009. Abc Transporters: The Power to Change. Nature Reviews Molecular Cell Biology 10, 218-27. https://doi.org/10.1038/nrm2646.

[42] Chaillou, Thomas, Kirby, Tyler J., and McCarthy, John J. 2014. Ribosome Biogenesis: Emerging Evidence for a Central Role in the Regulation of Skeletal Muscle Mass. Journal of Cellular Physiology 229, 1584-94. https://doi.org/https://doi.org/10.1002/jcp.24604.

[43] Qian, W. D., Wang, W. J., Zhang, J. N., et al. 2022. Exploitation of the Antifungal and Antibiofilm Activities of Plumbagin against *Cryptococcus Neoformans*. Biofouling 38, 558-74. https://doi.org/10.1080/08927014.2022.2094260.

[44] Xing, J. H., Nan, X., Cui, Q., et al. 2018. Nop-7-Associated 2 (Nsa2) Is Required for Ribosome Biogenesis and Protein Synthesis. Biochemical and Biophysical Research Communications 505, 249-54. https://doi.org/10.1016/j.bbrc.2018.09.041.

[45] Wang, H. X., Wang, Z. G., Xu, W. H., et al. 2021. Comprehensive Transcriptomic and Proteomic Analyses Identify Intracellular Targets for Myriocin to Induce *Fusarium Oxysporum* F. Sp.

Niveum Cell Death. Microbial Cell Factories 20, 15 69. https://doi.org/10.1186/s12934-021-01560-z.

[46] Lieschke, G. J., Oates, A. C., Crowhurst, M. O., et al. 2001. Morphologic and Functional Characterization of Granulocytes and Macrophages in Embryonic and Adult Zebrafish. Blood 98, 3087-96. https://doi.org/10.1182/blood.V98.10.3087.

[47] Li, F. M., Lv, Z. C., Zhong, Z. J., et al. 2023. The Effect of Cyclosporin a on *Aspergillus Niger* and the Possible Mechanisms Involved. Foods 12, 11 567. https://doi.org/10.3390/foods12030567.

[48] Abdelwahab, H., Del Campo, J. S. M., Dai, Y. M., et al. 2016. Mechanism of Rifampicin Inactivation in *Nocardia Farcinica*. Plos One 11, 23 e0162578. https://doi.org/10.1371/journal.pone.0162578.

[49] Gasmi, A., Bjorklund, G., Peana, M., et al. 2022. Phosphocalcic Metabolism and the Role of Vitamin D, Vitamin K2, and Nattokinase Supplementation. Critical Reviews in Food Science and Nutrition 62, 7062-71. https://doi.org/10.1080/10408398.2021.1910481.

[50] He, R. R., Zhong, Q. P., Chen, W. J., et al. 2023. Transcriptomic and Proteomic Investigation of Metabolic Disruption in *Listeria Monocytogenes* Triggered by Linalool and Its Application in Chicken Breast Preservation. Lwt-Food Science and Technology 176, 12 114492. https://doi.org/10.1016/j.lwt.2023.114492.

[51] Gao, C. B., Cai, X., Lymbery, A. J., et al. 2023. Integrative Transcriptomic Profiling Reveals the Key Pathways in the Regulation Mechanism of Fish Intestine-Spleen Immunity During the Bacterial Challenges. Aquaculture 568, 15 739320. https://doi.org/10.1016/j.aquaculture.2023.739320.

[52] Xu, C., Li, E. C., Suo, Y. T., et al. 2018. Histological and Transcriptomic Responses of Two Immune Organs, the Spleen and Head Kidney, in Nile Tilapia (Oreochromis Niloticus) to Long-Term Hypersaline Stress. Fish & Shellfish Immunology 76, 48-57. https://doi.org/10.1016/j.fsi.2018.02.041.

[53] Oikonomopoulou, K., Ricklin, D., Ward, P. A., et al. 2012. Interactions between Coagulation and Complement-Their Role in Inflammation. Seminars in Immunopathology 34, 151-65. https://doi.org/10.1007/s00281-011-0280-x.

[54] Pan, L. Y., Peng, C., Wang, L., et al. 2022. Network Pharmacology and Experimental Validation-Based Approach to Understand the Effect and Mechanism of Taohong Siwu Decoction against Ischemic Stroke. Journal of Ethnopharmacology 294, 12 115339. https://doi.org/10.1016/j.jep.2022.115339.

[55] Kobayashi, H., Albarracin, L., Sato, N., et al. 2016. Modulation of Porcine Intestinal Epitheliocytes Immunetranscriptome Response by Lactobacillus Jensenii Tl2937. Beneficial Microbes 7, 769-82. https://doi.org/10.3920/bm2016.0095.

[56] Krarup, A., Wallis, R., Presanis, J. S., et al. 2007. Simultaneous Activation of Complement and Coagulation by Mbl-Associated Serine Protease 2. Plos One 2, 8 e623. https://doi.org/10.1371/journal.pone.0000623.

[57] Xie, Y., Zhang, H. Z., and Huang, T. Q. 2022. Quantitative Proteomics Reveal Three Potential Biomarkers for Risk Assessment of Acute Myocardial Infarction. Bioengineered 13, 4939-50. https://doi.org/10.1080/21655979.2022.2037365.

[58] Ferluga, J., Kouser, L., Murugaiah, V., et al. 2017. Potential Influences of Complement Factor H in Autoimmune Inflammatory and Thrombotic Disorders. Molecular Immunology 84, 84-106. https://doi.org/10.1016/j.molimm.2017.01.015.

[59] Desai, J. V., Kumar, D., Freiwald, T., et al. 2023. C5a-Licensed Phagocytes Drive Sterilizing Immunity During Systemic Fungal Infection. Cell 186, 2802-+. https://doi.org/10.1016/j.cell.2023.04.031.

[60] de Willige, S. U., de Visser, M. C. H., Houwing-Duistermaat, J. J., et al. 2005. Genetic Variation in the Fibrinogen Gamma Gene Increases the Risk for Deep Venous Thrombosis by Reducing Plasma Fibrinogen Gamma ' Levels. Blood 106, 4176-83. https://doi.org/10.1182/blood-2005-05-2180.

[61] Wang, Y., Guo, W. J., Xie, S. X., et al. 2021. Multi-Omics Analysis of Brain Tissue Metabolome and Proteome Reveals the Protective Effect of Gross Saponins of *Tribulus Terrestris* L. Fruit against Ischemic Stroke in Rat. Journal of Ethnopharmacology 278, 11 114280. https://doi.org/10.1016/j.jep.2021.114280.

[62] Bryer, Scott C., Fantuzzi, Giamila, Van Rooijen, Nico, et al. 2008. Urokinase-Type Plasminogen Activator Plays Essential Roles in Macrophage Chemotaxis and Skeletal Muscle Regeneration1. The Journal of Immunology 180, 1179-88. https://doi.org/10.4049/jimmunol.180.2.1179.

[63] Das, Riku, Ganapathy, Swetha, Settle, Megan, et al. 2014. Plasminogen Promotes Macrophage Phagocytosis in Mice. Blood 124, 679-88. https://doi.org/10.1182/blood-2014-01-549659.

[64] Zhu, B. P., Zhou, J. C., Wang, Z. Q., et al. 2022. Interactions between Intestinal Morphology, Digestion, Inflammatory Responses, and Gut Microbiota of Juvenile Channel Catfish Elicited by Dietary Enzymatic Rice Protein. Fish & Shellfish Immunology 127, 155-65. https://doi.org/10.1016/j.fsi.2022.06.018.

[65] Xin, W. G., Li, X. D., Lin, Y. C., et al. 2022. Whole Genome Analysis of Host-Associated *Lactobacillus Salivarius* and the Effects on Hepatic Antioxidant Enzymes and Gut Microorganisms of *Sinocyclocheilus Grahami*. Frontiers in Microbiology 13, 15 1014970. https://doi.org/10.3389/fmicb.2022.1014970.

[66] Mirpuri, J., Raetz, M., Sturge, C. R., et al. 2014. Proteobacteria-Specific Iga Regulates Maturation of the Intestinal Microbiota. Gut Microbes 5, 28-39. https://doi.org/10.4161/gmic.26489.

[67] Khan, S., Godfrey, V., and Zaki, M. H. "Cytosolic Nucleic Acid Sensors in Inflammatory and Autoimmune Disorders." In *Nucleic Acid Sensing and Immunity, Pt A*, edited by C. VanpouilleBox and L. Galluzzi. International Review of Cell and Molecular Biology, 215-53. London: Academic Press Ltd-Elsevier Science Ltd, 2019.

[68] Minderman, M., Lantermans, H., van der Zwaan, C., et al. 2023. The Oncogenic Human B-Cell Lymphoma Myd88 L265p Mutation Genocopies Activation by Phosphorylation at the Toll/Interleukin-1 Receptor (Tir) Domain. Blood Cancer Journal 13, 10 125. https://doi.org/10.1038/s41408-023-00896-6.

[69] Wang, S. T., Zhang, K. L., Song, X. T., et al. 2023. Tlr4 Overexpression Aggravates Bacterial Lipopolysaccharide-Induced Apoptosis Via Excessive Autophagy and Nf-Kb/Mapk Signaling in Transgenic Mammal Models. Cells 12, 19 1769. https://doi.org/10.3390/cells12131769.

[70] Li, M., Xu, C. J., Li, D., et al. 2021. Transcriptome Analysis of the Spleen Provides Insight into the Immunoregulation of *Cyprinus Carpio* Koi under *Aeromonas Veronii* Infection. Aquaculture 540, 10 736650. https://doi.org/10.1016/j.aquaculture.2021.736650.

[71] Guo, J. J., Hu, X., Gao, Z. P., et al. 2021. Global Transcriptomic Response of *Listeria Monocytogenes* Exposed to Fingered Citron (*Citrus Medica* L. Var. *Sarcodactylis Swingle*) Essential Oil. Food Research International 143, 11 110274. https://doi.org/10.1016/j.foodres.2021.110274.

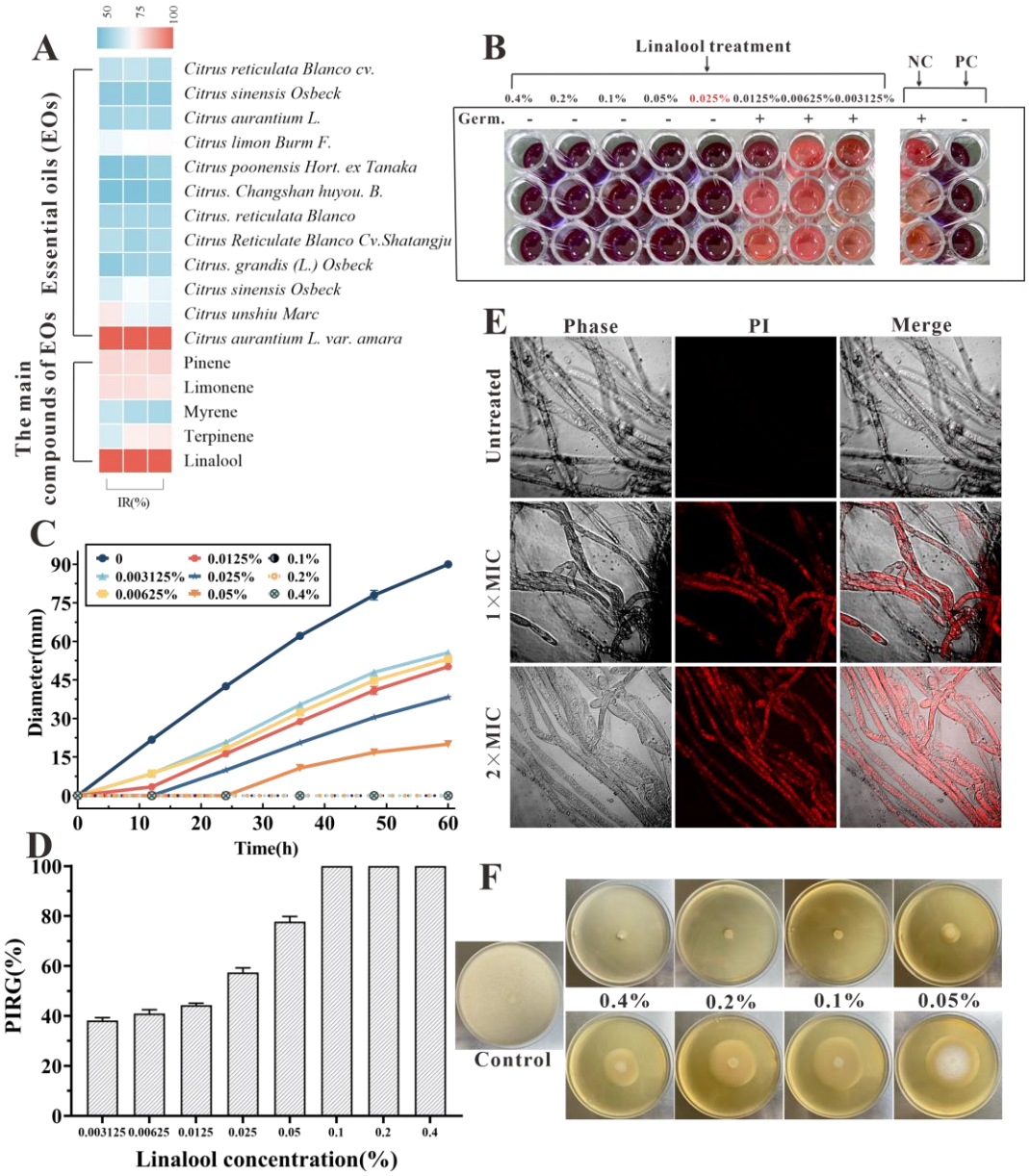

Figure 1. The *in vitro* anti-oomycetes activity of linalool against *S. parasitica* CQT2. A) Inhibition rate (IR) of EOs and their major components against *S. parasitica* CQT2. B) Determination of MIC of linalool against *S. parasitica* spores, employing malachite green (2.5 mg/mL) as a positive control (PC) and Tween 20 as a negative control (NC). C) Effects of linalool on mycelium growth inhibition over a 60h period at varying concentrations. D) Examination of the percentage inhibition of radial growth (PIRG %) in mycelium treated with linalool after 60 hours. E) Effects of linalool on the viability of *S. parasitica* CQT2 through a PI staining assay was conducted under 3 conditions:

982 Control (no linalool), 1×MIC (0.05%) linalool treatment, and 2×MIC (0.1%) linalool
983 treatment. F) Effects of different concentrations of linalool on mycelium growth on
984 PDA plates.

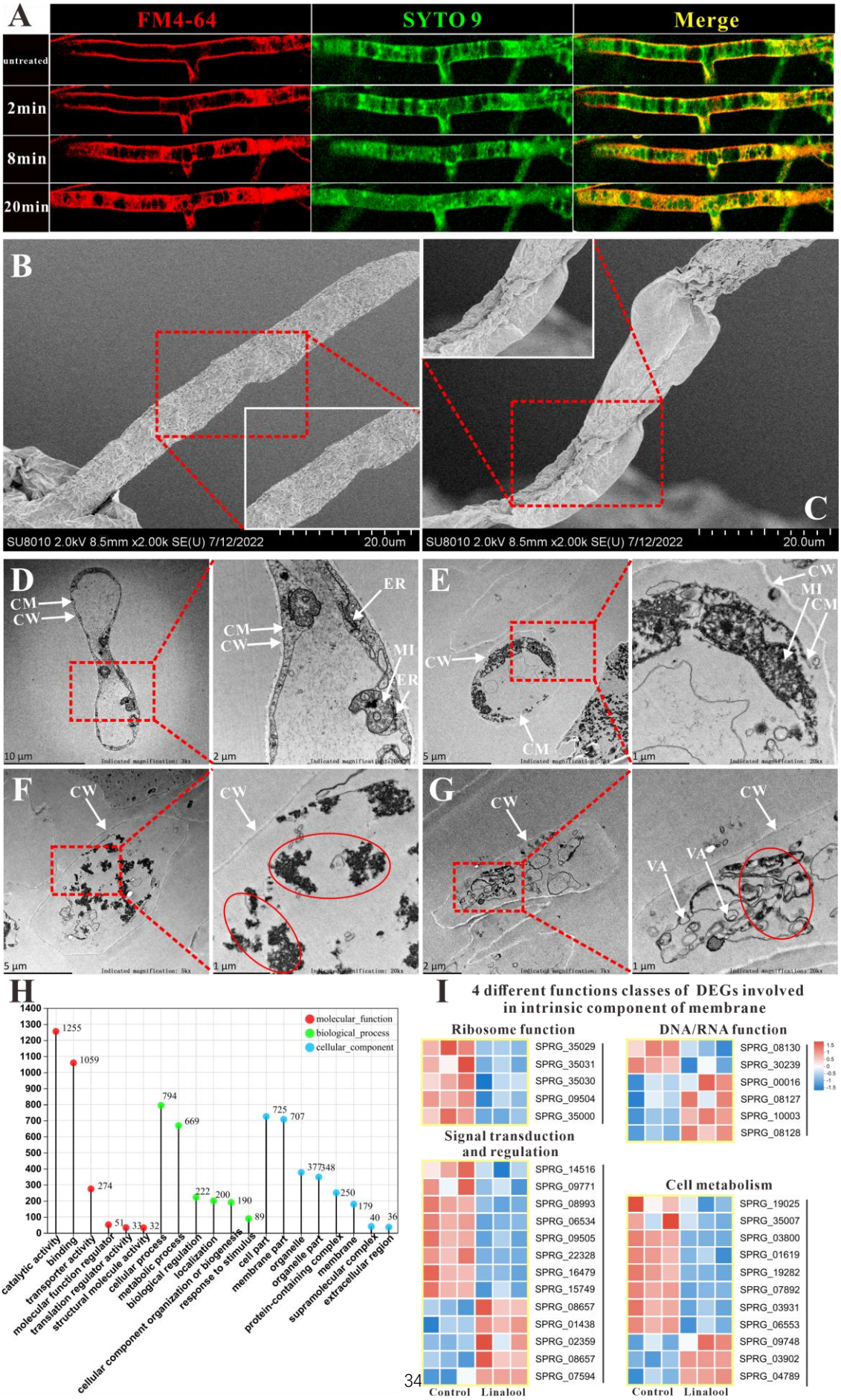
A
FM4-64
SYTO 9
Merge
untreated
2min
8min
20min
B
C
SU8010 2.0kV 8.5mm x2.00k SE(U) 7/12/2022
20.0um
D
CM
CW
ER
MI
10 μm
2 μm
E
CW
CM
MI
5 μm
1 μm
F
CW
5 μm
1 μm
G
CW
VA
2 μm
1 μm
H
molecular_function
biological_process
cellular_component
catalytic activity
binding
transporter activity
molecular function regulator
translation regulator activity
structural molecule activity
cellular process
metabolic process
biological regulation
localization
cellular component organization or biogenesis
response to stimulus
cell part
membrane part
organelle
organelle part
protein-containing complex
membrane
supramolecular complex
extracellular region
I
4 different functions classes of DEGs involved in intrinsic component of membrane
Ribosome function
SPRG_35029
SPRG_35031
SPRG_35030
SPRG_09504
SPRG_35000
DNA/RNA function
SPRG_08130
SPRG_30239
SPRG_00016
SPRG_08127
SPRG_10003
SPRG_08128
Signal transduction and regulation
SPRG_14516
SPRG_09771
SPRG_08993
SPRG_06534
SPRG_09505
SPRG_22328
SPRG_16479
SPRG_15749
SPRG_08657
SPRG_01438
SPRG_02359
SPRG_08657
SPRG_07594
Cell metabolism
SPRG_19025
SPRG_35007
SPRG_03800
SPRG_01619
SPRG_19282
SPRG_07892
SPRG_03931
SPRG_06553
SPRG_09748
SPRG_03902
SPRG_04789
Control
Linalool

985

986 **Figure 2**. Effects of linalool on the cell membrane integrity of *S. parasitica* CQT2. A)
987 Observation of the effect of linalool at 6×MIC (0.3%) on the cell membrane of *S.*
988 *parasitica* CQT2 using the FM4-64 and SYTO 9 staining assay. B-C) SEM images of
989 *S. parasitica* CQT2 mycelium without (no linalool, B) and with 1×MIC (0.05%, C)
990 linalool treatment. D-G) TEM images of *S. parasitica* CQT2 mycelium without (no
991 linalool, D) and with 1×MIC (0.05%, E-G) linalool treatment. CM: cell membrane; CW:
992 cell wall; ER: rough endoplasmic reticulum; MI: mitochondria; VA: vacuoles. H) The
993 GO classification of differentially expressed genes (DEGs). I) 4 different functions
994 classes (linked to ribosome function, involved in DNA/RNA function, connected to
995 signal transduction and regulation, and pertaining to cell metabolism) of differentially
996 expressed genes (DEGs) involved in intrinsic component of membrane.

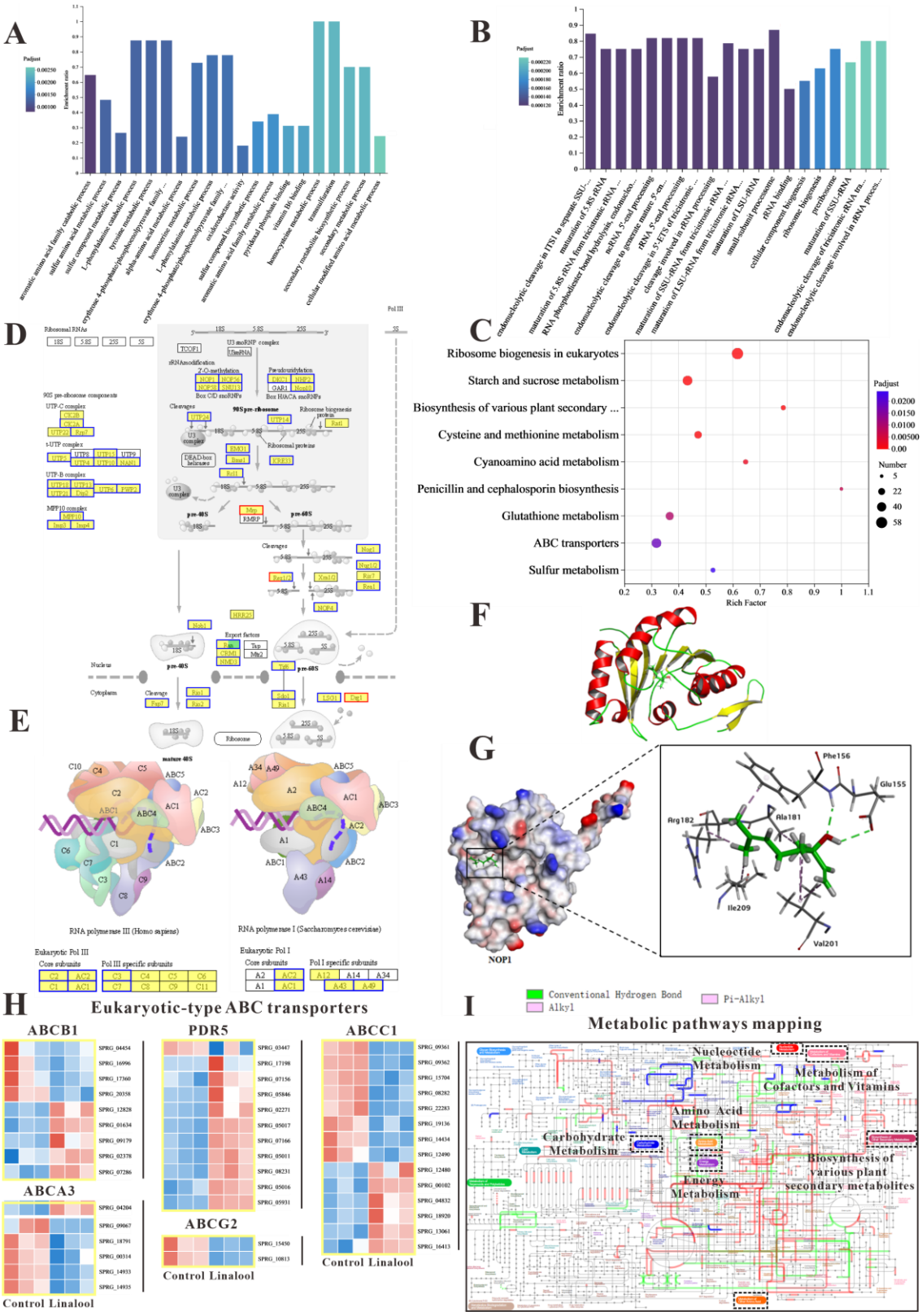

Figure 3. The *in vitro* anti-oomycete mechanisms revealed by transcriptome analysis. A-B) The GO enrichment of up and down regulated DEGs. C) The KEGG enrichment of DEGs. Significant enrichment was labeled as "*". $P < 0.05$, $P < 0.01$, and $P < 0.001$

1001 were labeled as “*”, “**”, and “***”, respectively. D) Comparison of ribosome
1002 biogenesis in eukaryotes pathway between the linalool treated mycelium and the control
1003 group. E) Comparison of RNA polymerase pathway between the linalool treated
1004 mycelium and the control group. F) The tertiary structure of NOP1 was displayed using
1005 a cartoon representation. G) Molecular docking of linalool with NOP1 was performed
1006 by enlarging the regions binding to the NOP1 activation pocket to showcase the detailed
1007 amino acid structures, which were presented using a surface model, while the small
1008 molecule was displayed with a ball-and-stick representation. H) Comparison of ABC
1009 transporters pathway between the linalool treated mycelium and the control group. The
1010 red squares represented up-regulated genes, and the blue squares represented down-
1011 regulated genes. I) Visual analysis of metabolic pathways with iPath3.0. The figure
1012 represented gene set annotated pathways, red and green represented pathways
1013 annotated by genes in different gene sets, respectively, and blue represented pathways
1014 co-annotated by genes in two gene sets.

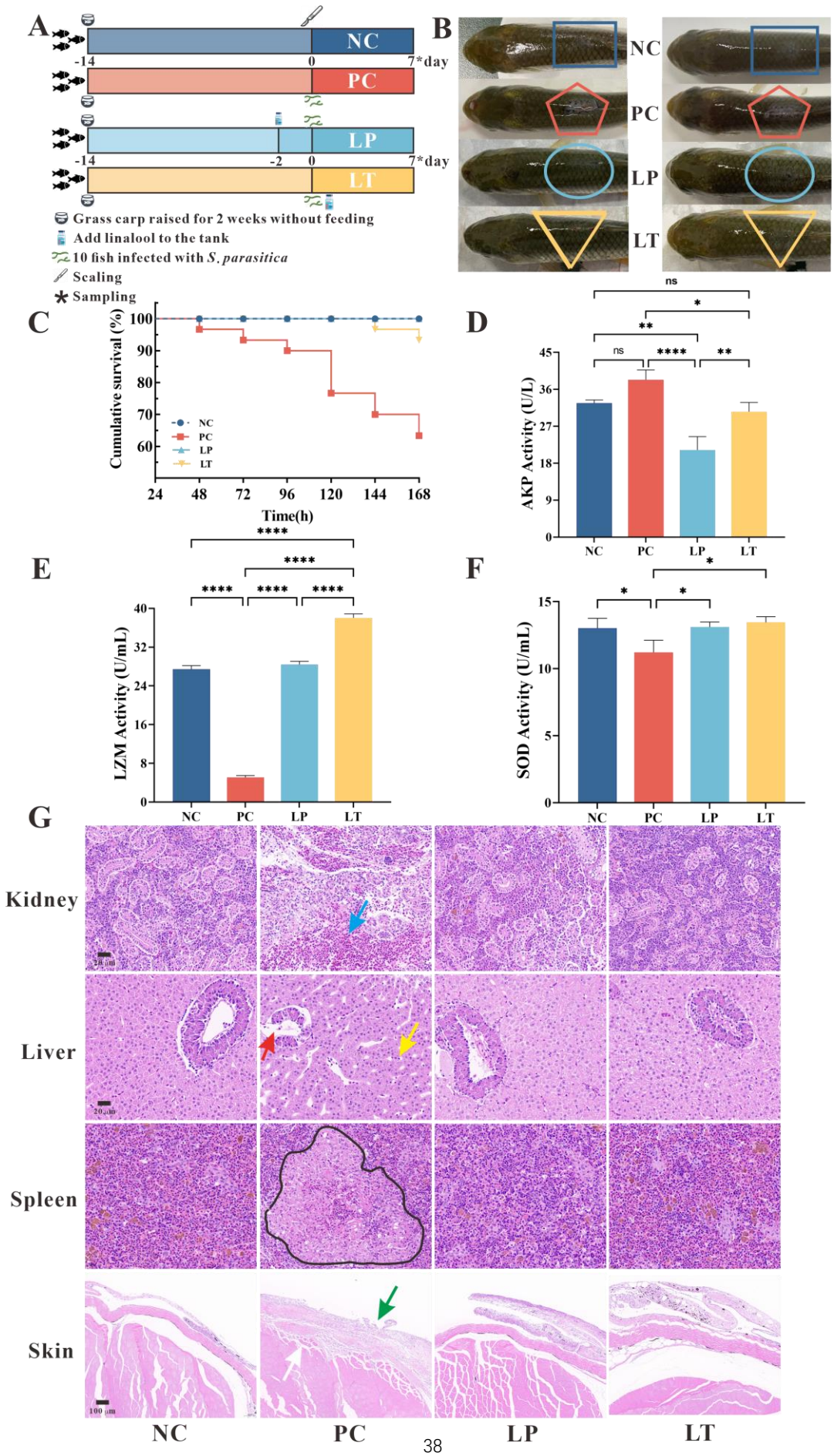
A
NC
PC
LP
LT
-14
0
7*day
-2
Grass carp raised for 2 weeks without feeding
Add linalool to the tank
10 fish infected with S. parasitica
Scaling
Sampling
B
NC
PC
LP
LT
C
Cumulative survival (%)
Time(h)
D
AKP Activity (U/L)
E
LZM Activity (U/mL)
F
SOD Activity (U/mL)
G
Kidney
Liver
Spleen
Skin
NC
PC
LP
LT

1016 **Figure 4.** Protective effect of linalool on grass carp infected with *S. parasitica*. A) The
1017 experimental design. Grass carp were raised for 2 weeks without feeding, fish without
1018 infection and linalool (negative control group, NC), fish infected with *S. parasitica*
1019 (positive control group, PC), and 10 fish uninfected soaked water containing linalool
1020 for 2 days and then 1×10^6 spores /mL secondary zoospores were added (linalool
1021 prophylactic group, LP), and fish infected with *S. parasitica* soaked for 7 days in water
1022 containing linalool (linalool therapeutic group, LT). B) The symptoms of *S. parasitica*
1023 infection in grass carps of different groups. C) The survival rates of grass carp infected
1024 with *S. parasitica* of different groups. D-F) Alkaline phosphatase (AKP), lysozyme
1025 (LYZ), and superoxide dismutase (SOD) activities in serum of grass carp of different
1026 groups. The results were presented as the means ± SD and were analyzed using one-
1027 way ANOVA followed by post hoc tests (*$p < 0.05$, **$p < 0.01$, ***$p < 0.001$, ****$p <$
1028 0.0001). G) Histopathological analysis grass carp tissues in different groups. The
1029 arrows of different colors indicated: inflammatory cell infiltration in the kidney (blue
1030 arrow), cytoplasmic pyknosis (red arrow), nuclei displaced toward one side (yellow
1031 arrow), the red and white pulp was poorly demarcated, and a larger volume of melano-
1032 macrophage centers (black area), critical damage to the epithelium (green arrow) and
1033 myofiber (white arrow).

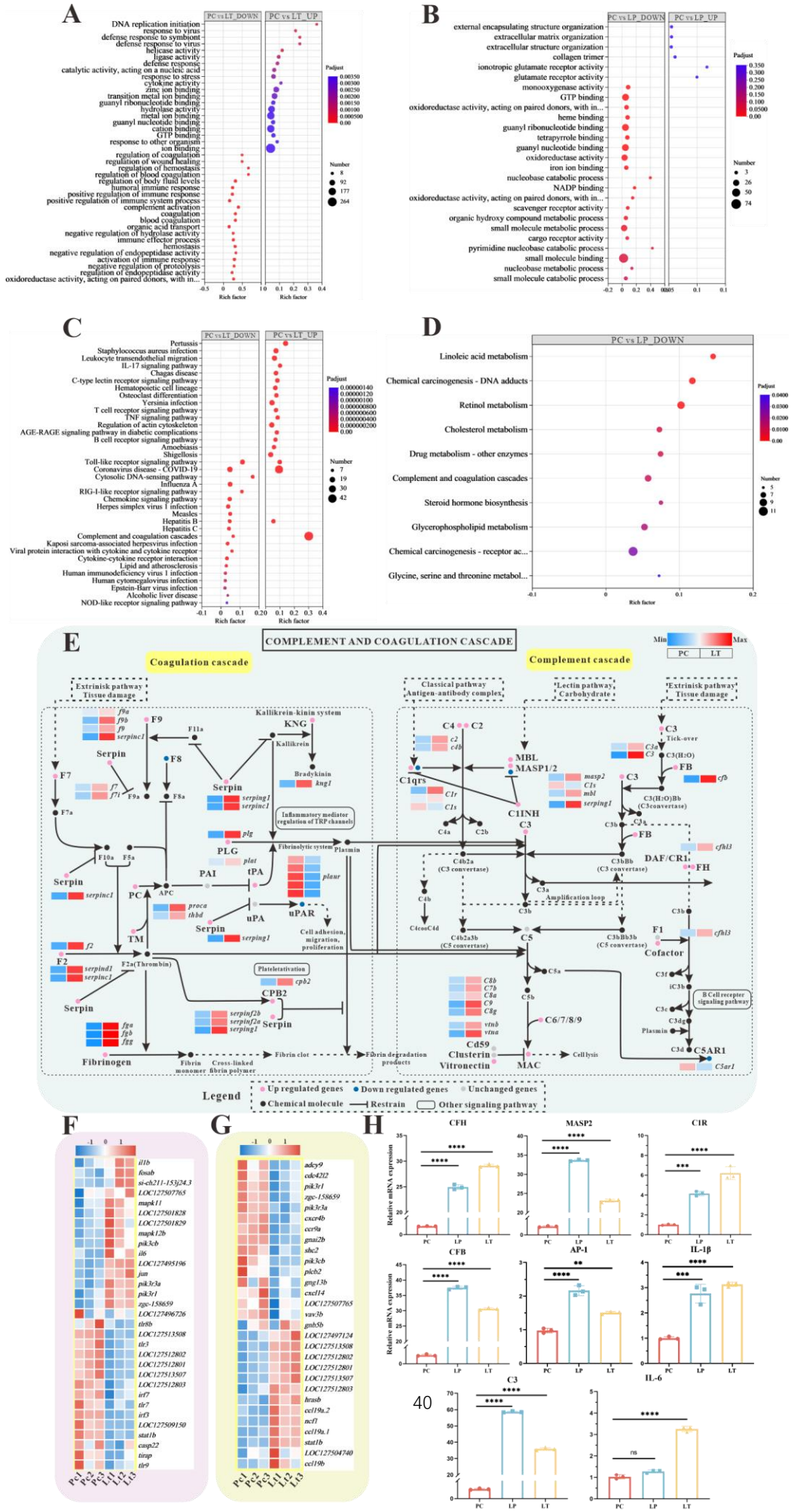
A
PC vs LT_DOWN
PC vs LT_UP
DNA replication initiation
response to virus
defense response to symbiont
defense response to virus
helicase activity
ligase activity
defense response
catalytic activity, acting on a nucleic acid
response to stress
cytokine activity
zinc ion binding
transition metal ion binding
guanyl ribonucleotide binding
hydrolase activity
metal ion binding
guanyl nucleotide binding
cation binding
GTP binding
response to other organism
ion binding
regulation of coagulation
regulation of wound healing
regulation of hemostasis
regulation of blood coagulation
regulation of body fluid levels
humoral immune response
positive regulation of immune response
positive regulation of immune system process
complement activation
coagulation
blood coagulation
organic acid transport
negative regulation of hydrolase activity
immune effector process
hemostasis
negative regulation of endopeptidase activity
activation of immune response
negative regulation of proteolysis
regulation of endopeptidase activity
oxidoreductase activity, acting on paired donors, with in...
Rich factor
Padjust
Number
B
PC vs LP_DOWN
PC vs LP_UP
external encapsulating structure organization
extracellular matrix organization
extracellular structure organization
collagen trimer
ionotropic glutamate receptor activity
glutamate receptor activity
monooxygenase activity
GTP binding
oxidoreductase activity, acting on paired donors, with in...
heme binding
guanyl ribonucleotide binding
tetrapyrrole binding
guanyl nucleotide binding
oxidoreductase activity
iron ion binding
nucleobase catabolic process
NADP binding
oxidoreductase activity, acting on paired donors, with in...
scavenger receptor activity
organic hydroxy compound metabolic process
small molecule metabolic process
cargo receptor activity
pyrimidine nucleobase catabolic process
small molecule binding
nucleobase metabolic process
small molecule catabolic process
Padjust
Number
C
PC vs LT_DOWN
PC vs LT_UP
Pertussis
Staphylococcus aureus infection
Leukocyte transendothelial migration
IL-17 signaling pathway
Chagas disease
C-type lectin receptor signaling pathway
Hematopoietic cell lineage
Osteoclast differentiation
Yersinia infection
T cell receptor signaling pathway
TNF signaling pathway
Regulation of actin cytoskeleton
AGE-RAGE signaling pathway in diabetic complications
B cell receptor signaling pathway
Amoebiasis
Shigellosis
Toll-like receptor signaling pathway
Coronavirus disease - COVID-19
Cytosolic DNA-sensing pathway
Influenza A
RIG-I-like receptor signaling pathway
Chemokine signaling pathway
Herpes simplex virus 1 infection
Measles
Hepatitis B
Hepatitis C
Complement and coagulation cascades
Kaposi sarcoma-associated herpesvirus infection
Viral protein interaction with cytokine and cytokine receptor
Cytokine-cytokine receptor interaction
Lipid and atherosclerosis
Human immunodeficiency virus 1 infection
Human cytomegalovirus infection
Epstein-Barr virus infection
Alcoholic liver disease
NOD-like receptor signaling pathway
Rich factor
Padjust
Number
D
PC vs LP_DOWN
Linoleic acid metabolism
Chemical carcinogenesis - DNA adducts
Retinol metabolism
Cholesterol metabolism
Drug metabolism - other enzymes
Complement and coagulation cascades
Steroid hormone biosynthesis
Glycerophospholipid metabolism
Chemical carcinogenesis - receptor ac...
Glycine, serine and threonine metabol...
Rich factor
Padjust
Number
E
COMPLEMENT AND COAGULATION CASCADE
Min
Max
PC
LT
Coagulation cascade
Complement cascade
Extrinisk pathway
Tissue damage
Classical pathway
Antigen-antibody complex
Lectin pathway
Carbohydrate
Extrinisk pathway
Tissue damage
Kallikrein-kinin system
KNG
Kallikrein
Bradykinin
Serpin
Inflammatory mediator regulation of TRP channels
Fibrinolytic system
Plasmin
PLG
PAI
tPA
uPA
uPAR
APC
PC
TM
F2a(Thrombin)
Plateletativation
CPB2
Cell adhesion, migration, proliferation
Fibrinogen
Fibrin monomer
Cross-linked fibrin polymer
Fibrin clot
Fibrin degradation products
C1qrs
C1INH
MBL
MASP1/2
C3
Tick-over
FB
DAF/CR1
FH
Amplification loop
C5
C6/7/8/9
Cd59
Clusterin
Vitronectin
MAC
Cell lysis
F1
Cofactor
B Cell recepter signaling pathway
Plasmin
C5AR1
Legend
Up regulated genes
Down regulated genes
Unchanged genes
Chemical molecule
Restrain
Other signaling pathway
F
G
H
CFH
MASP2
C1R
CFB
AP-1
IL-1β
C3
IL-6
Relative mRNA expression
PC
LP
LT
Pc1
Pc2
Pc3
Lt1
Lt2
Lt3

1034

1035 **Figure 5.** Global transcriptomic analysis after *S. parasitica* infection and linalool
1036 treatment in grass carp and in-depth analysis of crucial KEGG pathway and
1037 differentially expressed genes (DEGs). A-B) The GO enrichment of up and down
1038 regulated differentially expressed genes (DEGs) in linalool therapeutic (LT) and
1039 linalool prophylactic (LP) groups. C-D) The KEGG enrichment of up and down
1040 regulated differentially expressed genes (DEGs) in linalool therapeutic (LT) and
1041 linalool prophylactic (LP) groups. E) Complement and coagulation cascades pathway
1042 between *S. parasitica* infection and linalool treatment in the spleens of grass carp. F)
1043 31 differentially expressed genes (DEGs) related to Toll-like receptor signaling pathway.
1044 G) 29 differentially expressed genes (DEGs) related to chemokine signaling pathway.
1045 The red squares represented up-regulated genes, and the blue squares represented
1046 down-regulated genes. H) Expression levels of *cfh, masp2*, *c1r*, *c3*, *cfb*, *ap-1*, *il-1β*, and
1047 *il-6* in the spleen revealed variations among the PC, LP, and LT groups. For RT-qPCR,
1048 the results were presented as the means ± SD and were analyzed using independent t-
1049 tests (*$p < 0.05$, **$p < 0.01$, ***$p < 0.001$, ****$p < 0.0001$).

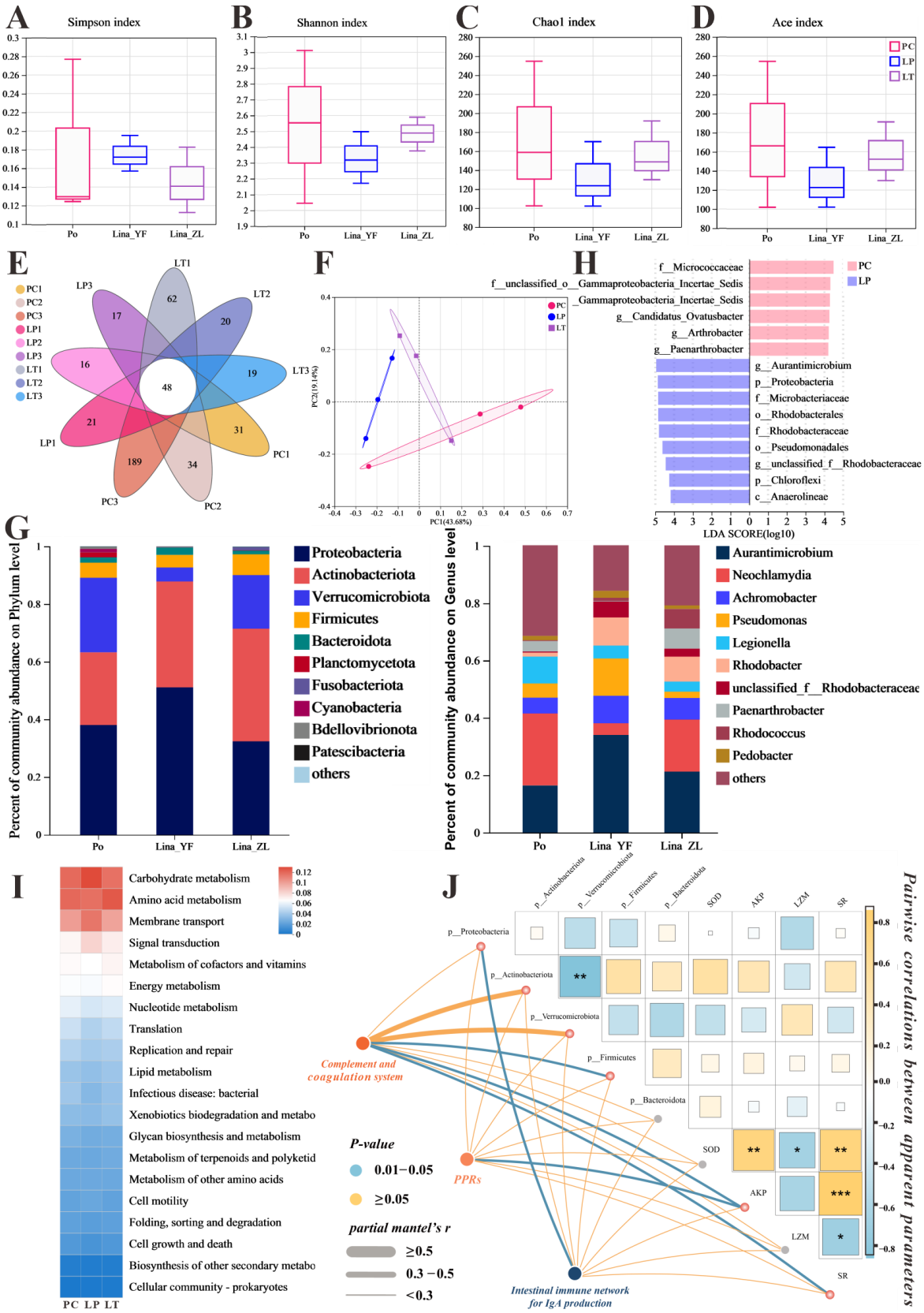

Figure 6. The effect of linalool on regulating gut microbiota of grass carp infected with *S. parasitica* and correlation analysis. A-D) The α diversity index comparison among the different groups. E) The OTUs petal map of positive control (PC), linalool

prophylactic (LP), and linalool therapeutic (LT) groups. F) PCoA using Bray–Curtis distance revealed variations among the positive control (PC), linalool prophylactic (LP), and linalool therapeutic (LT) groups (ANOSIM R = 0.3086, P = 0.061). G) Relative abundance of the top 10 species in the gut from the different groups (phylum and genus levels). H) Column chart of LDA value distribution. Discriminative biomarkers identified by linear discriminant analysis effect size (LEfSe) with logarithmic LDA score greater than 3.0. I) Heat map of the differences in predicted functional metabolisms within gut bacterial KEGG pathways. J) The correlation layout of potential related immune genes, specific microbial species, and physical characteristics. Pairwise comparisons of characterizations are presented, with a color gradient and block size denoting Pearson's correlation coefficients.

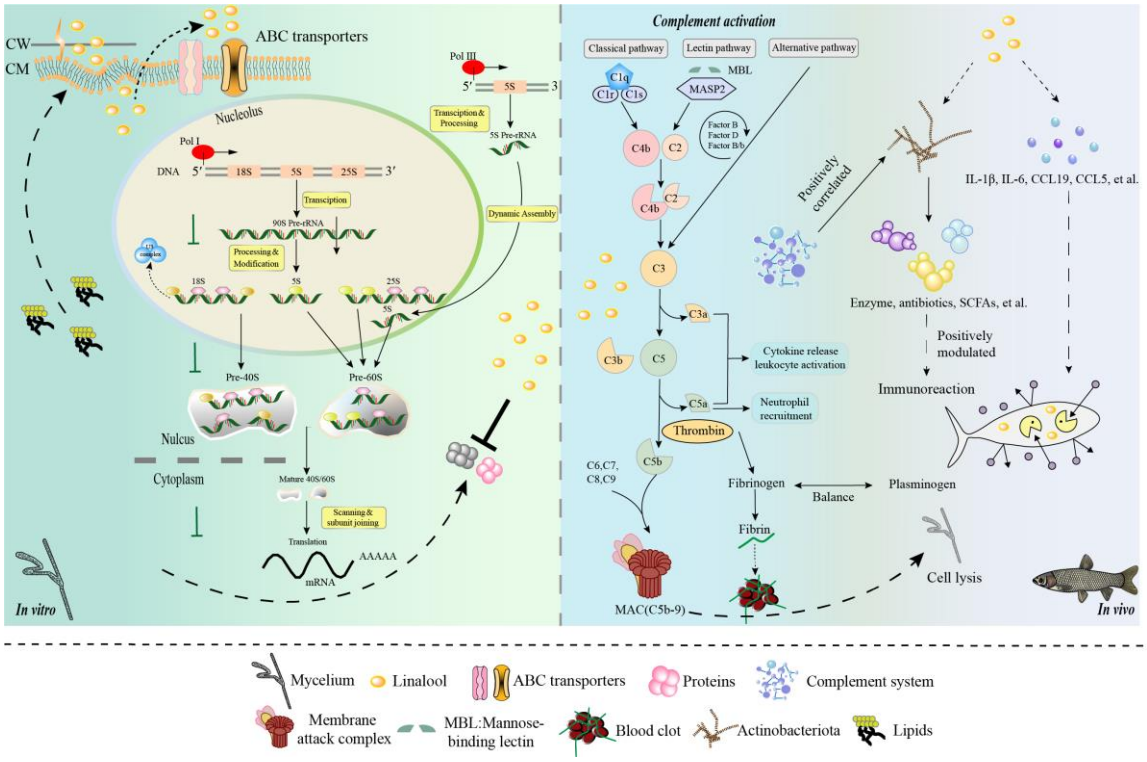

Figure 7. Model diagram of the mode of action of linalool on *S. parasitica* and grass carp. *In vitro*, (1) linalool influenced DNA transcription, tRNA transport, rRNA processing and maturation (5.8S, 18S, and 25S), and the biogenesis and assembly of ribosome subunits (40S and 60S) in the cell, which might lead to the reduction of S. parasitica growth; (2) Linalool disrupted the cell membrane, and the upregulation of glycerophospholipid metabolism likely represents the cell's response to cope with this

damage; (3) ABC transporters contributed to metabolic resistance by pumping linalool out of the cell. *In vivo*, (1) Linalool enhanced the complement and coagulation system which in turn activated host immune defense and lysate *S. parasitica* cells; (2) Linalool promoted wound healing, tissue repair, and phagocytosis to cope with *S. parasitica* infection; (3) Linalool positively modulated the immune response by increasing the abundance of beneficial Actinobacteriota; (4) Linalool stimulated the production of inflammatory cytokines (*il-1β* and *il-6*) and chemokines (*ccl19* and *ccl5)* to lyse *S. parasitica* cells.

Table 1. Primers for qPCR were used in this study.

Primer name	Primer sequence 5′-3′
c3-F	ACAAGCCCATCTACACGCCT
c3-R	GAAACCTCAGGAATGGCGTA
cfb-F	AGAATGGAGAGGTGACCCCA
cfb-R	CCGCTATCCTGACACACTCG
c1r-F	GGGTTTCGGAGGGTTTGA
c1r-R	CCTGTATTGCCACATCTTTCA
cfh-F	ATAGGAGGGAAATGTGGGC
cfh-R	TCCCGTCCACGCCATC
masp2-F	TGGGCACCAGGTTCATCG
masp2-R	GCTGTTTGACTACGCCCATCTT
il-1b-F	ATCTCCTCGTCTGCTGGGTG
il-1b-R	TTGAGAGTTTCAGTGACCTCCTTC
il-6-F	AAAATCTGACCTCAACCCTGG
il-6-R	TGTCCACCCTTCCTCTTGCT
ap-1-F	TCTCACTCAACAGATGCCAAAC
ap-1-R	CTTAGCGGCTGCGAGTTTAT
β-ActinF	GCTATGTGGCTCTTGACTTCG
β-ActinR	GGGCACCTGAACCTCTCATT

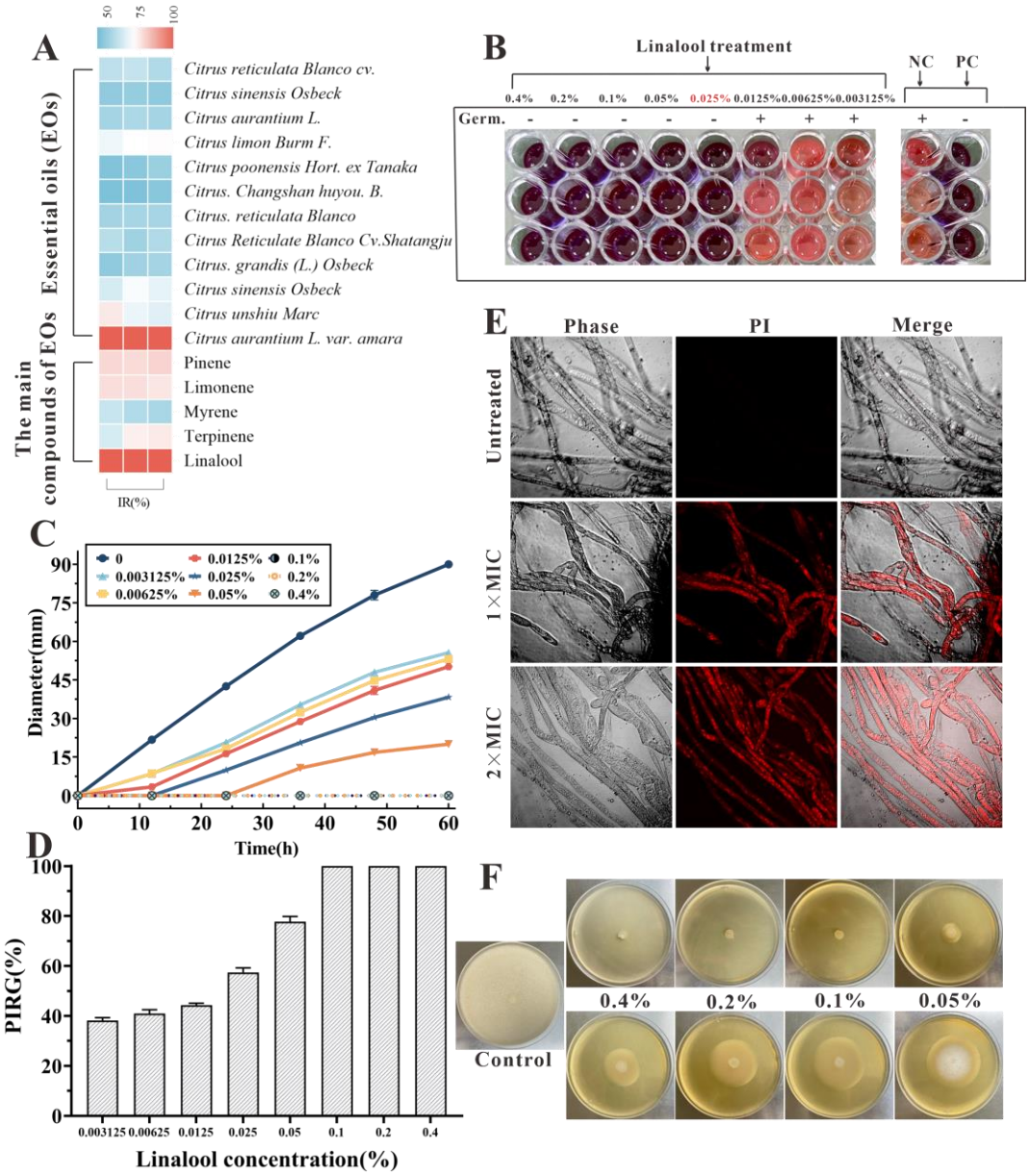

Figure 1. The *in vitro* anti-oomycetes activity of linalool against *S. parasitica* CQT2. A) Inhibition rate (IR) of EOs and their major components against *S. parasitica* CQT2. B) Determination of MIC of linalool against *S. parasitica* spores, employing malachite green (2.5 mg/mL) as a positive control (PC) and Tween 20 as a negative control (NC). C) Effects of linalool on mycelium growth inhibition over a 60h period at varying concentrations. D) Examination of the percentage inhibition of radial growth (PIRG %) in mycelium treated with linalool after 60 hours. E) Effects of linalool on the viability of *S. parasitica* CQT2 through a PI staining assay was conducted under 3 conditions: Control (no linalool), 1×MIC (0.05%) linalool treatment, and 2×MIC (0.1%) linalool

treatment. F) Effects of different concentrations of linalool on mycelium growth on PDA plates.

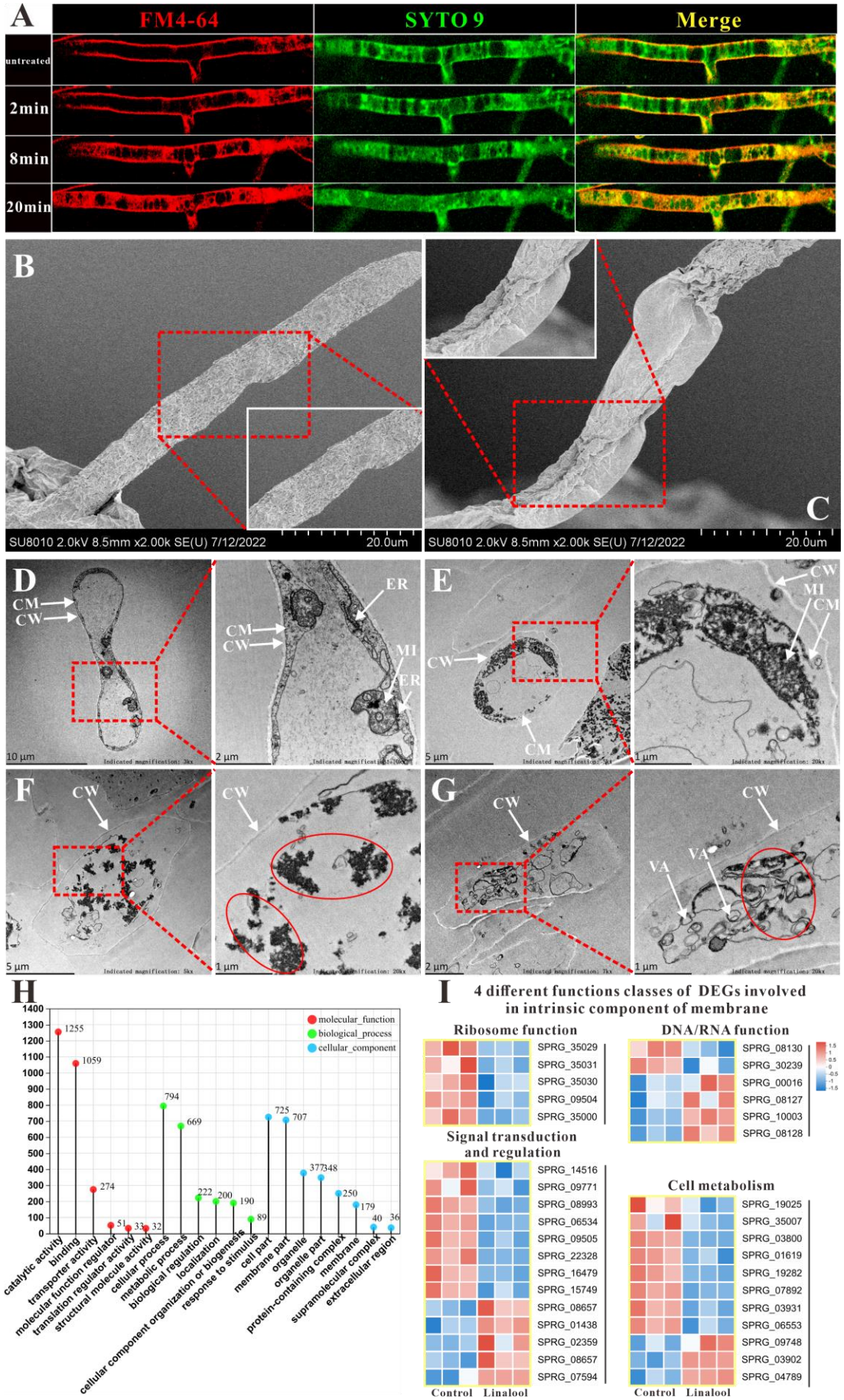
A
FM4-64
SYTO 9
Merge
untreated
2min
8min
20min
B
C
SU8010 2.0kV 8.5mm x2.00k SE(U) 7/12/2022
20.0um
D
CM
CW
ER
MI
E
F
G
VA
10 μm
2 μm
5 μm
1 μm
H
molecular_function
biological_process
cellular_component
catalytic activity
binding
transporter activity
molecular function regulator
translation regulator activity
structural molecule activity
cellular process
metabolic process
biological regulation
localization
cellular component organization or biogenesis
response to stimulus
cell part
membrane part
organelle
organelle part
protein-containing complex
membrane
supramolecular complex
extracellular region
I
4 different functions classes of DEGs involved in intrinsic component of membrane
Ribosome function
DNA/RNA function
Signal transduction and regulation
Cell metabolism
Control
Linalool

Figure 2. Effects of linalool on the cell membrane integrity of *S. parasitica* CQT2. A) Observation of the effect of linalool at 6×MIC (0.3%) on the cell membrane of *S. parasitica* CQT2 using the FM4-64 and SYTO 9 staining assay. B-C) SEM images of *S. parasitica* CQT2 mycelium without (no linalool, B) and with 1×MIC (0.05%, C) linalool treatment. D-G) TEM images of *S. parasitica* CQT2 mycelium without (no linalool, D) and with 1×MIC (0.05%, E-G) linalool treatment. CM: cell membrane; CW: cell wall; ER: rough endoplasmic reticulum; MI: mitochondria; VA: vacuoles. H) The GO classification of differentially expressed genes (DEGs). I) 4 different functions classes (linked to ribosome function, involved in DNA/RNA function, connected to signal transduction and regulation, and pertaining to cell metabolism) of differentially expressed genes (DEGs) involved in intrinsic component of membrane.

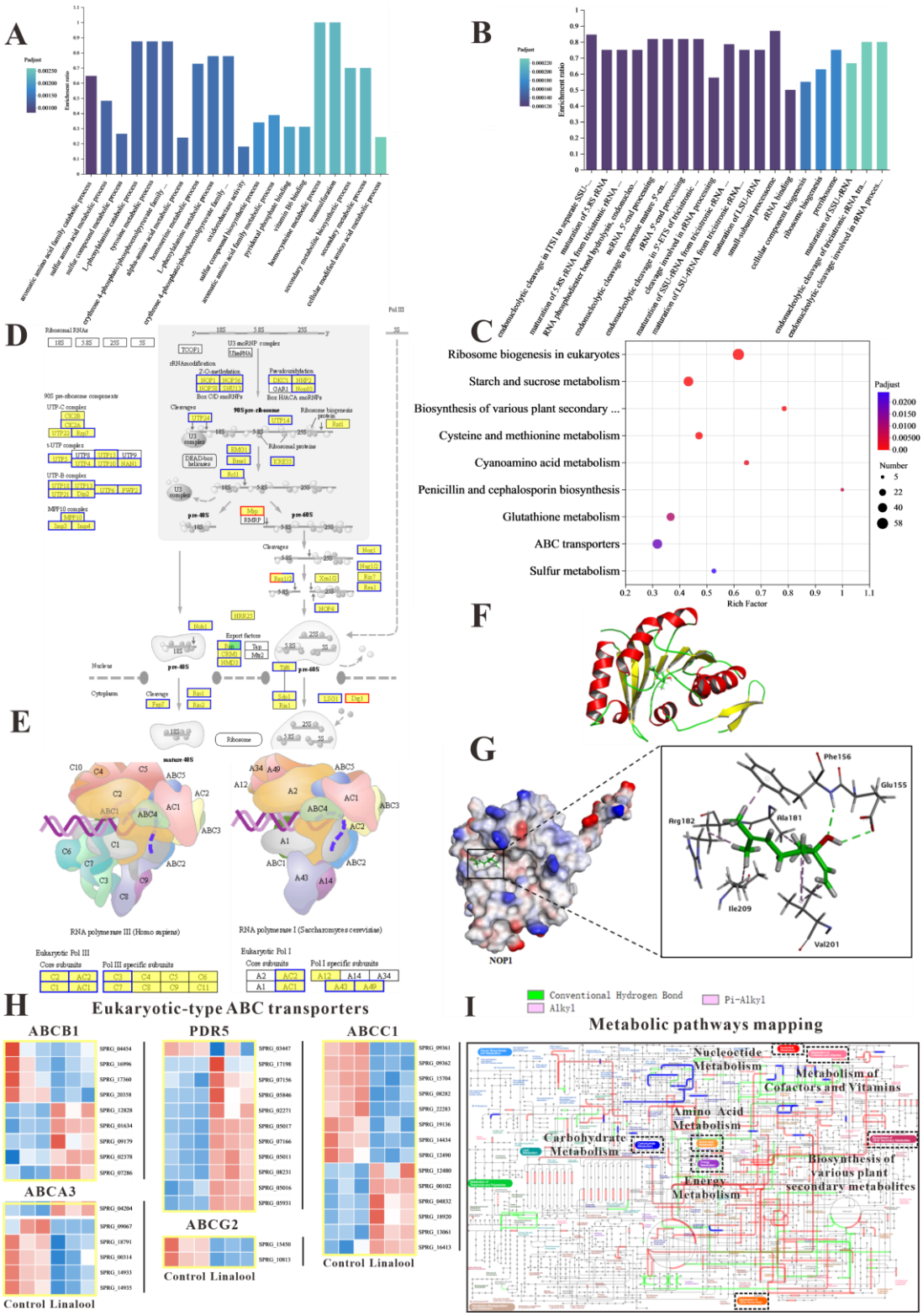

Figure 3. The *in vitro* anti-oomycete mechanisms revealed by transcriptome analysis. A-B) The GO enrichment of up and down regulated DEGs. C) The KEGG enrichment of DEGs. Significant enrichment was labeled as "*". $P < 0.05$, $P < 0.01$, and $P < 0.001$ were labeled as "*", "**", and "***", respectively. D) Comparison of ribosome

biogenesis in eukaryotes pathway between the linalool treated mycelium and the control group. E) Comparison of RNA polymerase pathway between the linalool treated mycelium and the control group. F) The tertiary structure of NOP1 was displayed using a cartoon representation. G) Molecular docking of linalool with NOP1 was performed by enlarging the regions binding to the NOP1 activation pocket to showcase the detailed amino acid structures, which were presented using a surface model, while the small molecule was displayed with a ball-and-stick representation. H) Comparison of ABC transporters pathway between the linalool treated mycelium and the control group. The red squares represented up-regulated genes, and the blue squares represented down-regulated genes. I) Visual analysis of metabolic pathways with iPath3.0. The figure represented gene set annotated pathways, red and green represented pathways annotated by genes in different gene sets, respectively, and blue represented pathways co-annotated by genes in two gene sets.

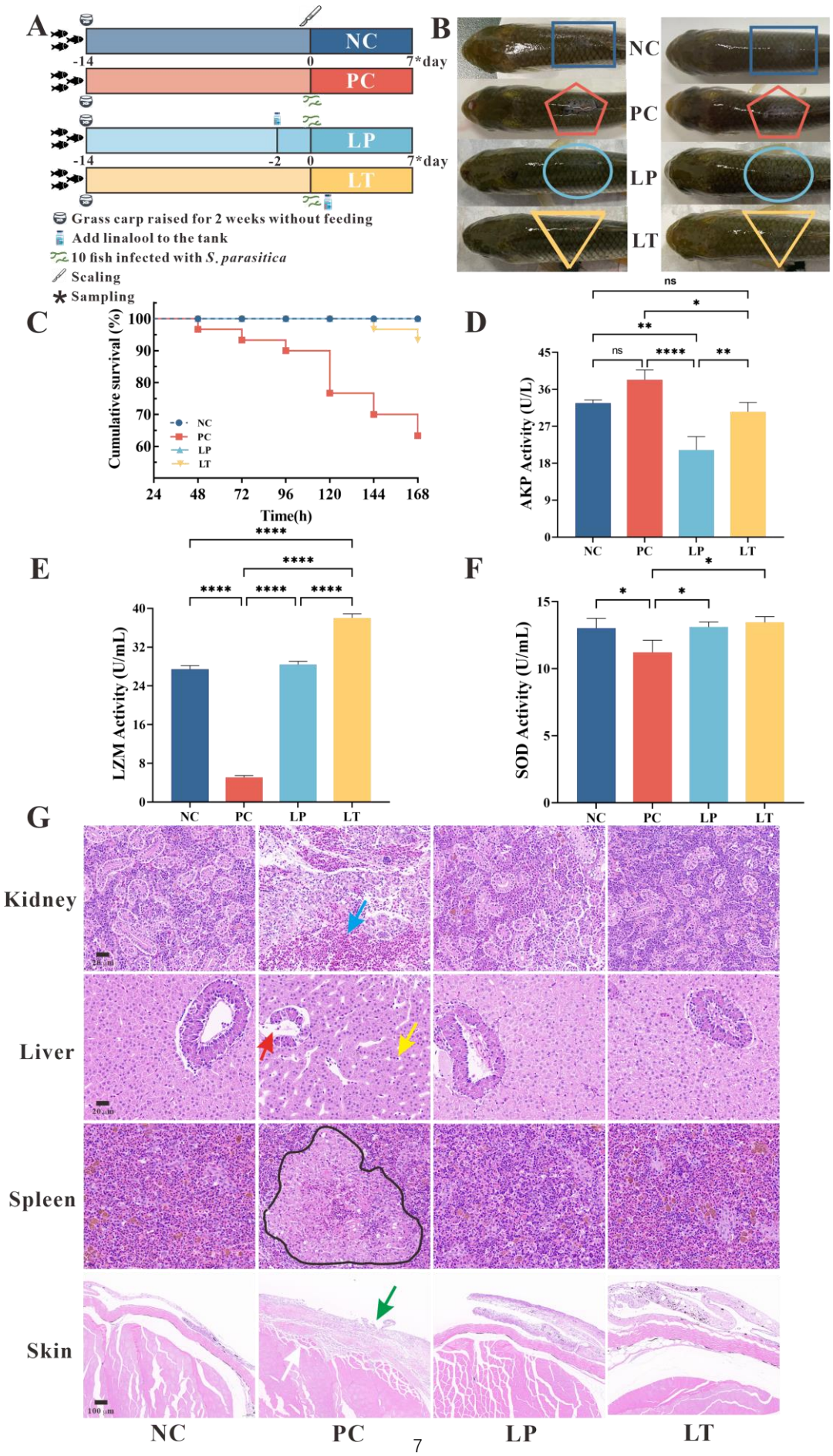
A
NC
PC
LP
LT
-14
0
7*day
-2
Grass carp raised for 2 weeks without feeding
Add linalool to the tank
10 fish infected with S. parasitica
Scaling
Sampling
B
NC
PC
LP
LT
C
Cumulative survival (%)
Time(h)
D
AKP Activity (U/L)
E
LZM Activity (U/mL)
F
SOD Activity (U/mL)
G
Kidney
Liver
Spleen
Skin
NC
PC
LP
LT

Figure 4. Protective effect of linalool on grass carp infected with *S. parasitica*. A) The experimental design. Grass carp were raised for 2 weeks without feeding, fish without infection and linalool (negative control group, NC), fish infected with *S. parasitica* (positive control group, PC), and 10 fish uninfected soaked water containing linalool for 2 days and then 1×10^6 spores /mL secondary zoospores were added (linalool prophylactic group, LP), and fish infected with *S. parasitica* soaked for 7 days in water containing linalool (linalool therapeutic group, LT). B) The symptoms of *S. parasitica* infection in grass carps of different groups. C) The survival rates of grass carp infected with *S. parasitica* of different groups. D-F) Alkaline phosphatase (AKP), lysozyme (LYZ), and superoxide dismutase (SOD) activities in serum of grass carp of different groups. The results were presented as the means ± SD and were analyzed using one-way ANOVA followed by post hoc tests (*$p < 0.05$, **$p < 0.01$, ***$p < 0.001$, ****$p < 0.0001$). G) Histopathological analysis grass carp tissues in different groups. The arrows of different colors indicated: inflammatory cell infiltration in the kidney (blue arrow), cytoplasmic pyknosis (red arrow), nuclei displaced toward one side (yellow arrow), the red and white pulp was poorly demarcated, and a larger volume of melano-macrophage centers (black area), critical damage to the epithelium (green arrow) and myofiber (white arrow).

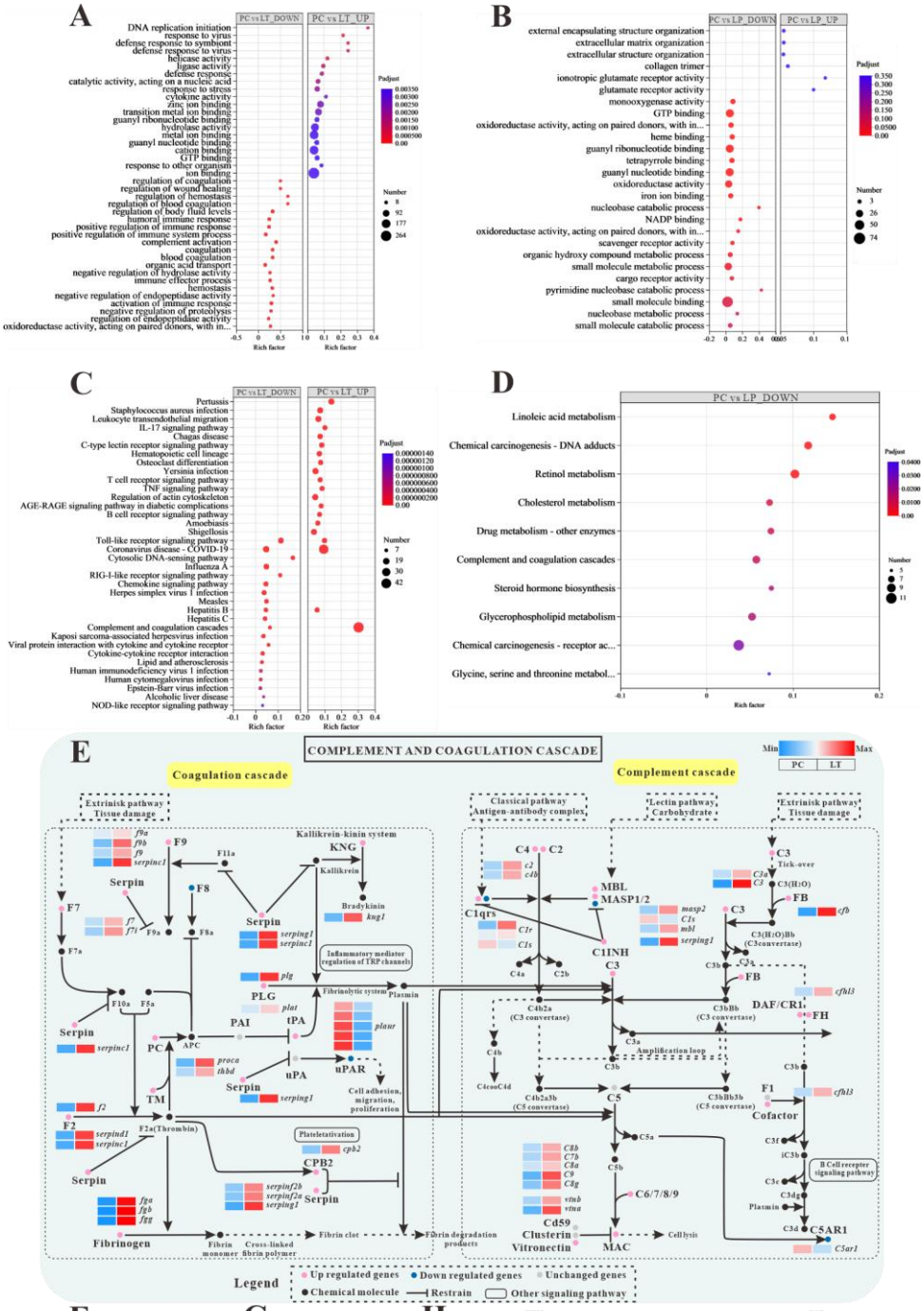
A
PC vs LT_DOWN
PC vs LT_UP
DNA replication initiation
response to virus
defense response to symbiont
defense response to virus
helicase activity
ligase activity
defense response
catalytic activity, acting on a nucleic acid
response to stress
cytokine activity
Zinc ion binding
transition metal ion binding
guanyl ribonucleotide binding
hydrolase activity
metal ion binding
guanyl nucleotide binding
cation binding
GTP binding
response to other organism
ion binding
regulation of coagulation
regulation of wound healing
regulation of hemostasis
regulation of blood coagulation
regulation of body fluid levels
humoral immune response
positive regulation of immune response
positive regulation of immune system process
complement activation
coagulation
blood coagulation
organic acid transport
negative regulation of hydrolase activity
immune effector process
hemostasis
negative regulation of endopeptidase activity
activation of immune response
negative regulation of proteolysis
regulation of endopeptidase activity
oxidoreductase activity, acting on paired donors, with in...
Rich factor
Padjust
Number
B
PC vs LP_DOWN
PC vs LP_UP
external encapsulating structure organization
extracellular matrix organization
extracellular structure organization
collagen trimer
ionotropic glutamate receptor activity
glutamate receptor activity
monooxygenase activity
GTP binding
oxidoreductase activity, acting on paired donors, with in...
heme binding
guanyl ribonucleotide binding
tetrapyrrole binding
guanyl nucleotide binding
oxidoreductase activity
iron ion binding
nucleobase catabolic process
NADP binding
oxidoreductase activity, acting on paired donors, with in...
scavenger receptor activity
organic hydroxy compound metabolic process
small molecule metabolic process
cargo receptor activity
pyrimidine nucleobase catabolic process
small molecule binding
nucleobase metabolic process
small molecule catabolic process
C
PC vs LT_DOWN
PC vs LT_UP
Pertussis
Staphylococcus aureus infection
Leukocyte transendothelial migration
IL-17 signaling pathway
Chagas disease
C-type lectin receptor signaling pathway
Hematopoietic cell lineage
Osteoclast differentiation
Yersinia infection
T cell receptor signaling pathway
TNF signaling pathway
Regulation of actin cytoskeleton
AGE-RAGE signaling pathway in diabetic complications
B cell receptor signaling pathway
Amoebiasis
Shigellosis
Toll-like receptor signaling pathway
Coronavirus disease - COVID-19
Cytosolic DNA-sensing pathway
Influenza A
RIG-I-like receptor signaling pathway
Chemokine signaling pathway
Herpes simplex virus 1 infection
Measles
Hepatitis B
Hepatitis C
Complement and coagulation cascades
Kaposi sarcoma-associated herpesvirus infection
Viral protein interaction with cytokine and cytokine receptor
Cytokine-cytokine receptor interaction
Lipid and atherosclerosis
Human immunodeficiency virus 1 infection
Human cytomegalovirus infection
Epstein-Barr virus infection
Alcoholic liver disease
NOD-like receptor signaling pathway
Rich factor
Padjust
Number
D
PC vs LP_DOWN
Linoleic acid metabolism
Chemical carcinogenesis - DNA adducts
Retinol metabolism
Cholesterol metabolism
Drug metabolism - other enzymes
Complement and coagulation cascades
Steroid hormone biosynthesis
Glycerophospholipid metabolism
Chemical carcinogenesis - receptor ac...
Glycine, serine and threonine metabol...
Rich factor
Padjust
Number
E
COMPLEMENT AND COAGULATION CASCADE
Coagulation cascade
Complement cascade
Min
Max
PC
LT
Extrinsic pathway
Tissue damage
Kallikrein-kinin system
KNG
Kallikrein
Bradykinin
Serpin
F7
F9
F8
F11a
F7a
F9a
F8a
F10a
F5a
PC
APC
TM
F2
F2a(Thrombin)
PLG
PAI
tPA
uPA
uPAR
Inflammatory mediator regulation of TRP channels
Fibrinolytic system
Plasmin
Cell adhesion, migration, proliferation
Plateletativation
CPB2
Fibrinogen
Fibrin monomer
Cross-linked fibrin polymer
Fibrin clot
Fibrin degradation products
Classical pathway
Antigen-antibody complex
Lectin pathway
Carbohydrate
C4
C2
C1qrs
C1r
C1s
C4a
C2b
MBL
MASP1/2
C1INH
C3
C3a
C3b
C4b
C4b2a
(C3 convertase)
C4b2a3b
(C5 convertase)
C5
C5a
C5b
C6/7/8/9
Cd59
Clusterin
Vitronectin
MAC
Cell lysis
Tick-over
C3(H2O)
FB
C3(H2O)Bb
(C3convertase)
C3bBb
(C3 convertase)
DAF/CR1
FH
Amplification loop
C3bBb3b
(C5 convertase)
F1
Cofactor
iC3b
C3c
C3dg
C3d
C5AR1
B Cell receptor signaling pathway
Legend
Up regulated genes
Down regulated genes
Unchanged genes
Chemical molecule
Restrain
Other signaling pathway
F
G
H
CFH
MASP2
C1R
CFB
AP-1
IL-1β
IL-6
C3
Relative mRNA expression
PC
LP
LT
ns

Figure 5. Global transcriptomic analysis after *S. parasitica* infection and linalool treatment in grass carp and in-depth analysis of crucial KEGG pathway and differentially expressed genes (DEGs). A-B) The GO enrichment of up and down regulated differentially expressed genes (DEGs) in linalool therapeutic (LT) and linalool prophylactic (LP) groups. C-D) The KEGG enrichment of up and down regulated differentially expressed genes (DEGs) in linalool therapeutic (LT) and linalool prophylactic (LP) groups. E) Complement and coagulation cascades pathway between *S. parasitica* infection and linalool treatment in the spleens of grass carp. F) 31 differentially expressed genes (DEGs) related to Toll-like receptor signaling pathway. G) 29 differentially expressed genes (DEGs) related to chemokine signaling pathway. The red squares represented up-regulated genes, and the blue squares represented down-regulated genes. H) Expression levels of *cfh, masp2*, *c1r*, *c3*, *cfb*, *ap-1*, *il-1β*, and *il-6* in the spleen revealed variations among the PC, LP, and LT groups. For RT-qPCR, the results were presented as the means ± SD and were analyzed using independent t-tests (*$p < 0.05$, **$p < 0.01$, ***$p < 0.001$, ****$p < 0.0001$).

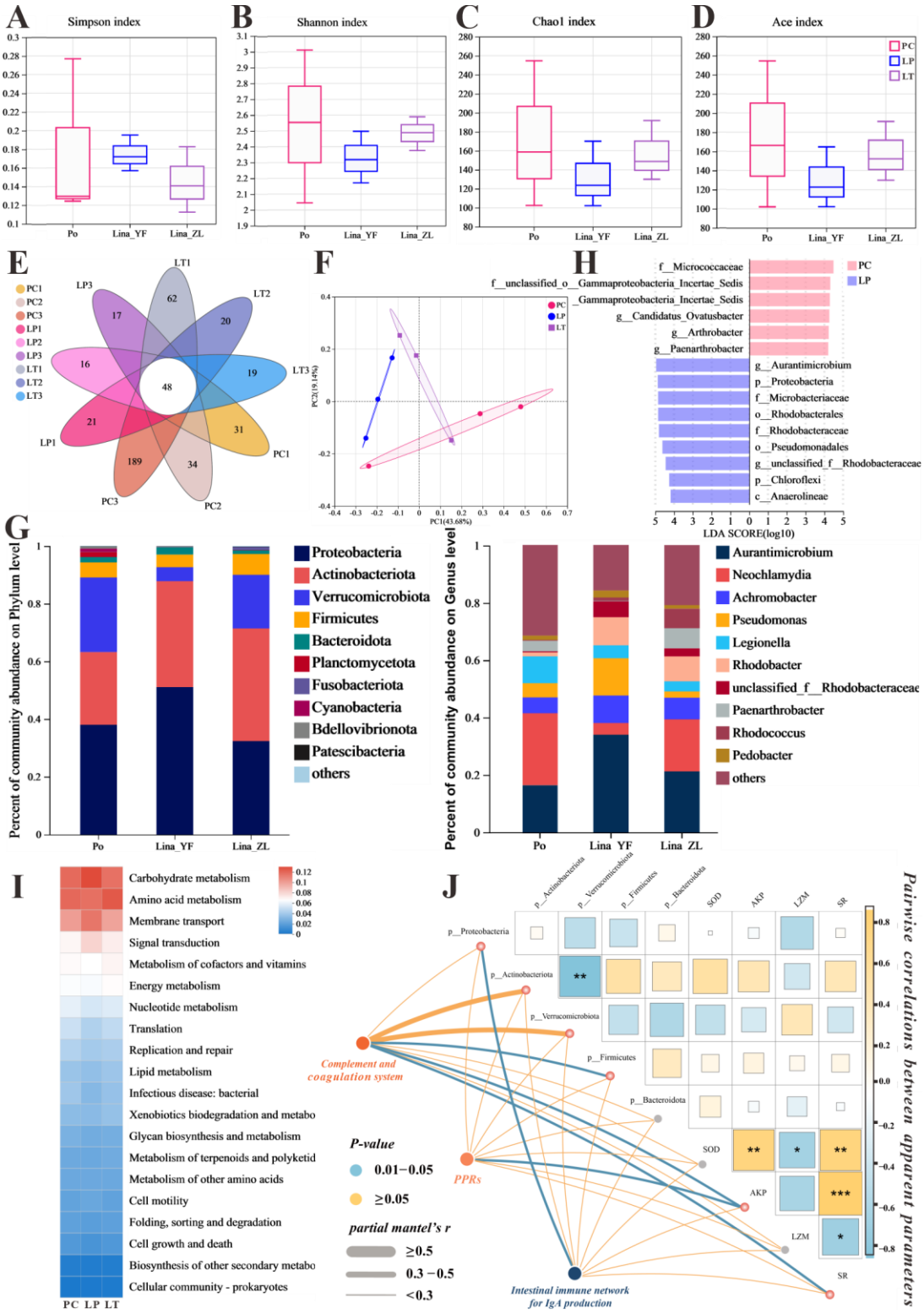

Figure 6. The effect of linalool on regulating gut microbiota of grass carp infected with *S. parasitica* and correlation analysis. A-D) The α diversity index comparison among the different groups. E) The OTUs petal map of positive control (PC), linalool prophylactic (LP), and linalool therapeutic (LT) groups. F) PCoA using Bray–Curtis

distance revealed variations among the positive control (PC), linalool prophylactic (LP), and linalool therapeutic (LT) groups (ANOSIM R = 0.3086, P = 0.061). G) Relative abundance of the top 10 species in the gut from the different groups (phylum and genus levels). H) Column chart of LDA value distribution. Discriminative biomarkers identified by linear discriminant analysis effect size (LEfSe) with logarithmic LDA score greater than 3.0. I) Heat map of the differences in predicted functional metabolisms within gut bacterial KEGG pathways. J) The correlation layout of potential related immune genes, specific microbial species, and physical characteristics. Pairwise comparisons of characterizations are presented, with a color gradient and block size denoting Pearson's correlation coefficients.

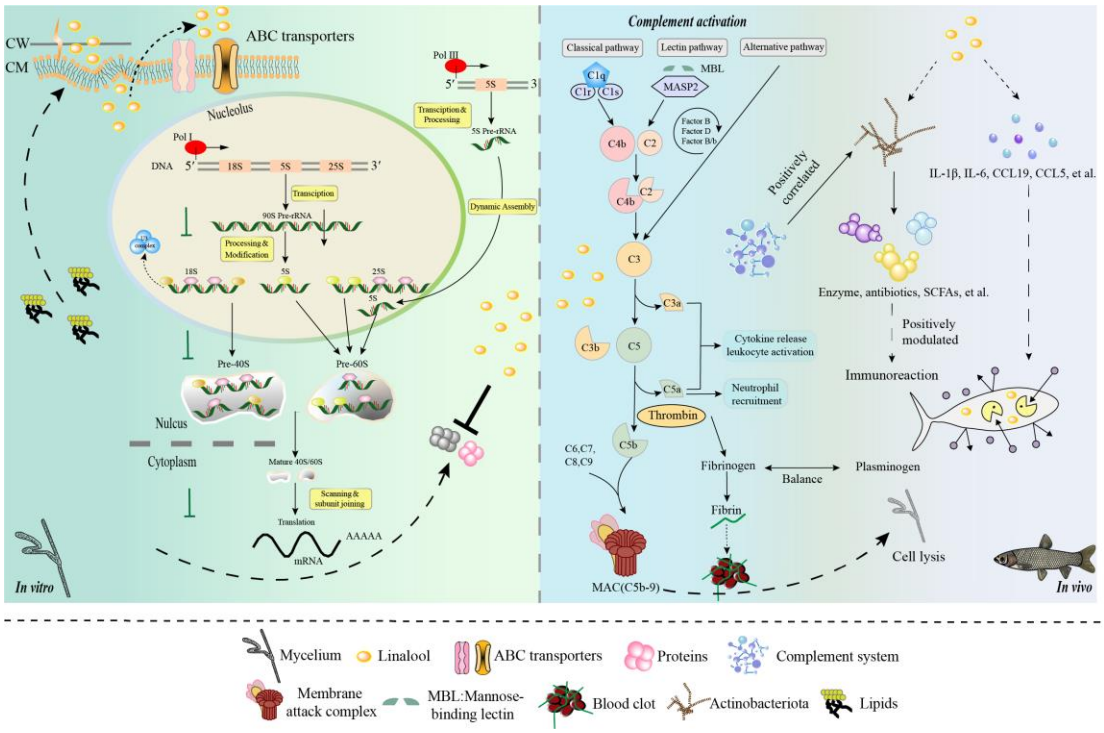

Figure 7. Model diagram of the mode of action of linalool on *S. parasitica* and grass carp. *In vitro*, (1) linalool influenced DNA transcription, tRNA transport, rRNA processing and maturation (5.8S, 18S, and 25S), and the biogenesis and assembly of ribosome subunits (40S and 60S) in the cell, which might lead to the reduction of S. parasitica growth; (2) Linalool disrupted the cell membrane, and the upregulation of glycerophospholipid metabolism likely represents the cell's response to cope with this damage; (3) ABC transporters contributed to metabolic resistance by pumping linalool out of the cell. *In vivo*, (1) Linalool enhanced the complement and coagulation system which in turn activated host immune defense and lysate *S. parasitica* cells; (2) Linalool promoted wound healing, tissue repair, and phagocytosis to cope with *S. parasitica* infection; (3) Linalool positively modulated the immune response by increasing the abundance of beneficial Actinobacteriota; (4) Linalool stimulated the production of inflammatory cytokines (*il-1β* and *il-6*) and chemokines (*ccl19* and *ccl5)* to lyse *S. parasitica* cells.